

Answers to the Referee

comments from referees/public:

L462-463: The higher vertical resolution of the previous study (Loginova et al. 2019) does not exclude a direct comparison with the present one, with lower vertical resolution. Why is not possible? I could understand it the other way around.

author's response:

We thank the reviewer for this comment and agree that a comparison between the loss rates based on a higher vertical sampling frequency (Loginova et al. 2019) and our dataset is possible. Our statement arose because a higher vertical resolution might have resulted in slightly different loss rates within our study. However, we will delete the questionable sentence and restrict the discussion to the different seasons and the labile DOM concentrations that are mentioned within the same paragraph.

author's changes in manuscript (page and line numbers refer to the revised manuscript pdf):

page 14 line 462

The sentence “Additionally, Loginova et al. (2019) sampled with a much higher vertical resolution within the upper 140 m, restricting the direct comparability with our study.” has been deleted.

comments from referees/public:

L465-470: Anammox has been proved to depend of the ammonium production by denitrification in the anoxic core (Babbin et al. 2014. Science 344, 406-408; Ward 2013. Science 341, 352-353.) and, due to the stoichiometry of the OM, only represent about 25-30% of the total rates. The presence of heterotrophic metabolism does not exclusively imply a dominance of denitrification as other processes (such as sulfate reduction, Candfield et al. 2010. Science 330, 1375-1378) might be equally relevant. It might be OK to later assume than the estimated rates are caused by denitrification, but this study does not provide clear evidences to show “the widespread occurrence of heterotrophic denitrification processes in the Peruvian OMZ”.

author's response:

We are grateful for this comment and included a possible contribution of sulfate reduction to heterotrophic anaerobic processes within this paragraph. We further mention the general dominance of denitrification in relation to anammox, based on the stoichiometry of organic matter

author's changes in manuscript (page and line numbers refer to the revised manuscript pdf):

page 14 line 466

“Studies based on the stoichiometry of organic matter suggest a general dominance of denitrification in relation to anammox and relate variable ratios between these two processes to the stoichiometry of locally available organic matter (Babbin et al., 2014; Ward, 2013). Our study points towards a widespread occurrence of heterotrophic anaerobic processes such as denitrification or sulfate reduction (Canfield et al., 2010) in the Peruvian OMZ, since the here applied method for measuring bacterial production is restricted to heterotrophs.”

38 **Bacterial degradation activity in the Eastern Tropical South**

39 **Pacific oxygen minimum zone**

40 Marie Maßmig, Jan Lüdke, Gerd Krahnann, Anja Engel*

41 GEOMAR Helmholtz Centre for Ocean Research Kiel, Düsternbrooker Weg 20, D-24105 Kiel, Germany

42 *Correspondence to:* Anja Engel (aengel@geomar.de)

43 **Abstract.** Oxygen minimum zones (OMZs) show distinct biogeochemical processes that relate to microorganisms
44 being able to thrive under low or even absent oxygen. Microbial degradation of organic matter is expected to be
45 reduced in OMZs, although quantitative evidence is low. Here, we present heterotrophic bacterial production (³H
46 leucine-incorporation), extracellular enzyme rates (leucine aminopeptidase /β-glucosidase) and bacterial cell
47 abundance for various *in situ* oxygen concentrations in the water column, including the upper and lower oxycline, of
48 the Eastern Tropical South Pacific off Peru. Bacterial heterotrophic activity in the suboxic core of the OMZ (at *in*
49 *situ* ≤5 μmol O₂ kg⁻¹) ranged from 0.3 to 281 μmol C m⁻³ d⁻¹ and was not significantly lower than in waters of 5-60
50 μmol O₂ kg⁻¹. Moreover, bacterial abundance in the OMZ and leucine aminopeptidase activity were significantly
51 higher in suboxic waters compared to waters of 5-60 μmol O₂ kg⁻¹, suggesting no impairment of bacterial organic
52 matter degradation in the core of the OMZ. Nevertheless, high cell-specific bacterial production was observed in
53 samples from oxyclines and cell-specific extracellular enzyme rates were especially high at the lower oxycline,
54 corroborating earlier findings of highly active and distinct micro-aerobic bacterial communities. To assess the impact
55 of bacterial degradation of dissolved organic matter (DOM) for oxygen loss in the Peruvian OMZ, we compared
56 diapycnal fluxes of oxygen and dissolved organic carbon (DOC) and their microbial uptake within the upper 60_m of
57 the water column. Our data indicate low bacterial growth efficiencies of 1-21% at the upper oxycline, resulting in a
58 high bacterial oxygen demand that can explain up to 33% of the observed average oxygen loss over depth. Our study
59 therewith shows that microbial degradation of DOM has a considerable share in sustaining the OMZ off Peru.

60 1. Introduction

61 In upwelling zones at eastern continental margins, oxygen minimum zones (OMZs) with hypoxic ($<60 \mu\text{mol O}_2 \text{ kg}^{-1}$)
62 ¹), suboxic ($<5 \mu\text{mol O}_2 \text{ kg}^{-1}$) or even anoxic conditions occur (Gruber, 2011; Thamdrup et al., 2012; Tiano et al.,
63 2014). OMZs have expanded over the past years resulting in an $\sim 3.7\%$ increase of hypoxic waters at depth (200
64 dbar) between 1960 and 2008 (Stramma et al., 2010). One of the largest anoxic water masses in the global ocean (2.4
65 $\times 10^{13} \text{ m}^3$) is located in the Eastern Tropical South Pacific and includes the Peruvian upwelling system (Kämpf and
66 Chapman, 2016; Paulmier and Ruiz-Pino, 2009; Thamdrup et al., 2012). There, nutrient-rich water is upwelled and
67 supports high rates of primary production and accumulation of organic matter. Biological degradation of organic
68 matter subsequently reduces oxygen below the surface mixed layer (Kämpf and Chapman, 2016). As a consequence,
69 and supported by sluggish ventilation of water masses, a permanent OMZ forms between 100 and 500 m depth, with
70 upper and lower boundaries, i.e. oxyclines, varying within seasonal and inter-annual cycles (Czeschel et al., 2011;
71 Graco et al., 2017; Kämpf and Chapman, 2016). In austral winter, upwelling and subsequently the nutrient supply to
72 the surface waters increase (Bakund and Nelson, 1991; Echevin et al., 2008). However, chlorophyll *a* (Chl *a*)
73 concentration is highest in austral summer, with the seasonal amplitude being stronger for surface than for depth
74 averaged Chl *a* concentrations (Echevin et al., 2008). In winter, phytoplankton growth is, next to iron, mainly
75 limited by light due to the deeper mixing, whereas in summer macronutrients can become a limiting factor (Echevin
76 et al., 2008). Further, El Niño–Southern Oscillation may affect organic matter cycling in the area since it affects the
77 depth of the oxycline and therefore the extent of anaerobic processes in the upper water column (Llanillo et al.,
78 2013). During the year of this study (2017), neither a strong La Niña nor a strong El Niño was detected
79 (<https://ggweather.com/enso/oni.htm>). However, in January, February and March 2017 there was a strong coastal El
80 Niño with enhanced warming ($+1.5^\circ\text{C}$) of sea surface temperatures in the eastern Pacific (Garreaud, 2018).

81 Within OMZs, enhanced vertical carbon export has been observed (Devol and Hartnett, 2001; Roullier et al., 2014)
82 and explained by a potentially reduced remineralization of organic matter in suboxic and anoxic waters. This is
83 possibly because microbes apply anaerobic respiratory pathways that yield less metabolic energy compared to
84 aerobic respiration. For instance, denitrification or dissimilatory nitrate reduction to ammonia (DNRA) result only in
85 99 %, or 64 % of the energy (kJ) per oxidized carbon atom that is produced by aerobic respiration (Lam and
86 Kuypers, 2011). Additionally, the energy yield available for the production of cell mass seems to be less than
87 expected from the chemical equations (Strohm et al., 2007). Meanwhile, bacteria are mainly responsible for the
88 remineralization of organic matter into nutrients and carbon dioxide (CO_2) in the ocean (Azam et al., 1983). Thus,
89 microbial activity and consequently organic matter remineralization in suboxic and anoxic waters might be reduced,
90 possibly explaining enhanced export of carbon. As a consequence, expanding OMZs could result in increased CO_2
91 storage in the ocean.

92 During the degradation process, low molecular weight (LMW $<1 \text{ kDa}$) organic compounds can directly be taken up
93 by bacteria (Azam et al., 1983; Weiss et al., 1991). However, in the ocean, bioavailable organic matter is commonly
94 in the form of particulate organic matter or high molecular weight (HMW) DOM (Benner and Amon, 2015). To
95 access this organic matter pool, bacteria produce extracellular, substrate specific enzymes that hydrolyse polymers

96 into LMW units (Hoppe et al., 2002). Taken-up, organic matter is partly incorporated into bacterial biomass, or
97 respired to CO₂, which may evade to the atmosphere (Azam et al., 1983). Rates of enzymatic organic matter
98 hydrolysis or bacterial production are controlled by the environment, i.e. temperature and pH, but can be actively
99 regulated e.g. in response to changing organic matter supply and quality (Boetius and Lochte, 1996; Grossart et al.,
100 2006; Pantoja et al., 2009; Piontek et al., 2014). However, the effect of oxygen concentration, which dictates the
101 respiratory pathway and thus energy gain, on bacterial production and the expression of extracellular enzymes in
102 aquatic systems, is poorly understood. For instance, bacterial production was higher in anoxic lake waters (Cole and
103 Pace, 1995), whereas in the Pacific waters off Chile bacterial production and DOM decomposition rates did not
104 change in relation to oxygen concentrations (Lee, 1992; Pantoja et al., 2009). Investigations of hydrolysis rates as the
105 initial step of organic matter degradation, may help to unravel possible adaptation strategies of bacterial communities
106 to suboxic and anoxic conditions (Hoppe et al., 2002). High extracellular enzyme rates might compensate a putative
107 lower energy yield of anaerobic respiration and the subsequent biogeochemical effects. However, very few studies
108 have investigated the effect of oxygen on hydrolytic rates, so far. Hoppe et al. (1990) did not find differences
109 between oxic and anoxic incubations of Baltic Sea water. In the Cariaco Basin, hydrolytic rates were significantly
110 higher in oxic compared to anoxic water (Taylor et al., 2009). However, this difference did not persist after rates
111 were normalized to particulate organic matter concentration. The dependence of hydrolysis rates on organic matter
112 concentrations described by Taylor et al. (2009), suggest that productivity may play a role for extracellular
113 enzymatic rates in oxygen depleted systems. The Peruvian upwelling system displays high amounts of labile organic
114 matter (Loginova et al., 2019) at shallow oxyclines and thus allows for studying effects of low oxygen on
115 extracellular enzyme rates under substrate replete conditions. In general, combined investigations of extracellular
116 enzyme rates, bacterial production (measured by ³H leucine-incorporation) and carbon fluxes sampled at various *in*
117 *situ* oxygen concentrations are still missing. These data, however, are crucial to inform ocean biogeochemical
118 models that aim at quantification of CO₂ uptake and nitrogen loss processes in oxygen depleted areas.

119 We studied bacterial degradation of organic matter in the OMZ off Peru during an extensive sampling campaign in
120 the Austral winter 2017. We determined rates of total and cell-specific bacterial production (³H leucine-
121 incorporation) as well as of leucine aminopeptidase (LAPase) and β-glucosidase (GLUCase). We estimate bacterial
122 utilisation of DOC supplied by diapycnal transport into the OMZ and discuss the contribution of bacterial
123 degradation activity to the formation and persistence of the OMZ off Peru.

124 2. Methods

125 2.1. Study site and CTD measurements

126 Samples were taken during the cruises M136 and M138 on the R/V METEOR off Peru in April and June 2017,
127 respectively (Fig. 1). Seawater was sampled with 24 Niskin bottles (10 L) on a general oceanic rosette system. At
128 each station, 5 to 11 depths were sampled between 3 and 800 m (supplementary Table 1). Oxygen concentrations,
129 temperature and depth were measured with a Sea-Bird SBE 9-plus CTD System (Sea-Bird Electronics, Inc., USA).
130 Oxygen concentrations at each depth were determined with a SBE 43 oxygen sensor, calibrated with Winkler
131 titrations (Winkler, 1888), resulting in an overall accuracy of 1.5 μmol kg⁻¹ oxygen. Chl *a* fluorescence was detected

132 with a WETStar Chl *a* sensor (WET Labs, USA) and converted to $\mu\text{g l}^{-1}$ using factors given by the manufacturer
133 (Wetlabs).

134 **2.2. Dissolved organic carbon, total dissolved nitrogen, dissolved hydrolysable amino** 135 **acids and dissolved high molecular weight carbohydrates**

136 DOC and total dissolved nitrogen (TDN) samples were taken at all stations, whereas the further analysis of DOC
137 data was limited to stations with compatible bacterial production data and turbulence measurements (stations G-T).
138 For DOC and TDN 20 ml of seawater was sampled in replicates, whereas both replicates were only analysed in case
139 of conspicuous data. Samples were filtered through a syringe filter (0.45 μm glass microfiber GD/X membrane,
140 Whatman TM) that was rinsed with 50 ml sample, into a combusted glass ampoule (8 h, 500 °C). Before sealing the
141 ampoules, 20 μl of 30 % ultrapure hydrochloric acid were added. Samples were stored at 4 °C in the dark for 3 months
142 until analyses. DOC and TDN were analysed using a TOC-VCSH with a TNM-1 detector (Shimadzu), applying a
143 high-temperature catalytic oxidation method modified from Sugimura and Suzuki (1988). The instrument was
144 calibrated with potassium hydrogen phthalate standard solutions (0 to 416.7 $\mu\text{mol C l}^{-1}$) (Merck 109017) and a
145 potassium nitrate standard solution (0-57.1 $\mu\text{mol N l}^{-1}$) (Merck 105065). The instrument blank was examined with
146 reference seawater standards (Hansell laboratory RSMAS University of Miami). The relative standard deviation
147 (RSD) between repeated measurements is <1.1 % and <3.6 % and the detection limit is 1 $\mu\text{mol l}^{-1}$ and 2 $\mu\text{mol l}^{-1}$ for
148 DOC and TDN, respectively.

149 At each station replicate 4 ml and 16 ml sample for the analysis of dissolved amino acids (DHAA) and dissolved
150 combined carbohydrates (DCHO) were filtered through rinsed Acrodisc® 0.45 μm GHP membrane (Pall) and stored
151 in combusted vials (8 h, 500 °C) at -20 °C, respectively. Replicates were only analysed, if the first sample analyses
152 resulted conspicuous data. The following DHAA were analysed: Alanine, Arginine, Glycine, Leucine,
153 Phenylalanine, Serine, Threonine, Tyrosine, Valine, Aspartic acid + Asparagine (co-eluted), Glutamine + Glutamic
154 acid (co-eluted), γ -Aminobutyric acid and Isoleucine. DHAA samples were analysed with a high performance liquid
155 chromatograph (1260 HPLC system, Agilent Technologies) using a C₁₈ column (Phenomex Kinetex) after in line
156 ortho-phthaldialdehyde derivatization with mercaptoethanol after Lindroth and Mopper (1979) and Dittmar et al.
157 (2009) with slight modifications after Engel and Galgani (2016). DCHO samples were desalted by membrane
158 dialysis (1kDa, Spectra Por) and analysed with a high performance anion exchange chromatography (HPAEC)
159 (DIONEX ICS3000DC) after Engel and Händel (2011). Detection limit of DHAA was 1.4 nmol L⁻¹ depending on
160 amino acid and 10 nmol L⁻¹ for DCHO. The precision was 2% and 5% for DHAA and DCHO, respectively.

161 **2.3. Diapycnal fluxes of oxygen and dissolved organic carbon**

162 In this study, we calculated DOC and oxygen loss rates ($\text{mmol m}^{-3} \text{d}^{-1}$) from the changes in diapycnal fluxes over
163 depth. Therefore, oxygen and DOC profiles were used (stations G-T), excluding the mixed layer, defined by
164 temperature deviating $\leq 0.2^\circ\text{C}$ from the maximum, but excluding at least the upper 10 m. The diapycnal flux (Φ_s)
165 was calculated for each CTD profile (Fischer et al., 2013; Schafstall et al., 2010) assuming a constant gradient
166 between two sampled depths for DOC and oxygen:

167 $1. \quad \Phi_S = -K_\rho \nabla C_S$

168 where ∇C_S is the gradient (mol m^{-4}). The diapycnal diffusivity of mass (K_ρ) ($\text{m}^2 \text{s}^{-1}$) was assumed to be constant
 169 ($10^{-3} \text{m}^2 \text{s}^{-1}$), which is reasonable compared with turbulence measurements by a freefalling microstructure probe
 170 (see supplementary methods and Fig. 2a). DOC loss rates ($\nabla \Phi_{DOC}$; $\text{mmol m}^{-3} \text{d}^{-1}$) and oxygen loss rates ($\nabla \Phi_{DO}$; mmol
 171 $\text{m}^{-3} \text{d}^{-1}$) were assumed to be equal to the negative vertical divergence of Φ_S calculated from the mean diapycnal flux
 172 profile, implying all other physical supply processes to be negligible.

173 **2.4. Bacterial abundance**

174 Bacterial abundance was sampled in replicates at each station, whereas replicates were only analysed in exceptions.
 175 Abundance was determined by flow cytometry after Gasol and Del Giorgio (2000) from 1.6 ml sample, fixed with
 176 0.75 μl 25 % glutaraldehyde on board and stored at -80°C for maximal 3 month until analyses. Prior to analysis
 177 samples were thawed and 10 μL Fluoresbrite® fluorescent beads (Polyscience, Inc.) and 10 μL Sybr Green
 178 (Invitrogen) (final concentration: 1x of the 1000x Sybr Green concentrate) were added to 400 μl sample. Cells were
 179 counted on a FACS Calibur (Becton Dickinson), calibrated with TruCount Beads™ (BD) with a measurement error
 180 of 2 % RSD.

181 **2.5. Bacterial production, oxygen demand and growth efficiency**

182 For bacterial production, the incorporation of radioactive labelled leucine (^3H) (specific activity 100 Ci mmol^{-1} ,
 183 Biotrend) was measured (Kirchman et al., 1985; Smith and Azam, 1992) at all depths of stations G-T as replicates.
 184 For this, the radiotracer at a saturating final concentration of 20 nmol l^{-1} was added to 1.5 ml of sample and incubated
 185 for 3 hours in the dark at 13°C . Controls were poisoned with trichloroacetic acid. Samples were measured with a
 186 liquid scintillation counter (Hidex 300 SL, Triathaler™, FCI). Samples taken at *in situ* oxygen concentrations of < 5
 187 $\mu\text{mol kg}^{-1}$ were incubated under anoxic conditions by gentle bubbling with gas (0.13 % CO_2 in pure N_2). Samples
 188 from oxic waters were incubated with head space, without bubbling. All samples were shaken thoroughly in
 189 between, therefore the bubbling of just one treatment won't have any effect. ^3H -leucine uptake was converted to
 190 carbon units applying a conversion factor of 1.5 kg C mol^{-1} leucine (Simon and Azam, 1989). An analytical error of
 191 5.2 % RSD was estimated with triplicate calibrations. Samples with a SD (standard deviation) $> 30\%$ between
 192 replicates were excluded.

193 The incubation of samples at a constant temperature of 13°C resulted in deviations of max. 11°C between incubation
 194 ($T_{incubation}$) and *in situ* temperatures (T_{insitu}). In order to estimate *in situ* bacterial production from measured bacterial
 195 production during incubations, measured temperature differences were taken into account following the approach of
 196 López-Urrutia and Morán (2007). First, the temperature difference between T_{insitu} and $T_{incubation}$ (δT) was computed in
 197 electron volt (eV^{-1}), after T_{insitu} and $T_{incubation}$ (K) had been multiplied with the Boltzmann's constant k ($8.62 \times 10^{-5} \text{eV K}$
 198 $^{-1}$):

199 $2. \quad \delta T [\text{eV}^{-1}] = \frac{1}{T_{incubation}[\text{K}] \times k [\text{eV K}^{-1}]} - \frac{1}{T_{insitu}[\text{K}] \times k [\text{eV K}^{-1}]}$

200 The decadal logarithm of *in situ* bacterial production ($\log_{10} BP_{in situ}$) was then calculated from the decadal logarithm of
 201 measured bacterial production during incubations ($\log_{10} BP_{incubation}$). Therefore we applied three different factors (F)
 202 depending on *in situ* Chl *a* concentration as proposed by López-Urrutia and Morán (2007); with F being -0.583, -0.5
 203 and -0.42 [$fgCcell^{-1}d^{-1}ev$] for <0.5, 0.5-2 and >2 μg Chl *a* L^{-1} , respectively:

204

205 3. $\log_{10} BP_{in situ} [fgCcell^{-1}d^{-1}] =$

$$\log_{10} BP_{incubation} [fgCcell^{-1}d^{-1}] + \delta T [ev^{-1}] \times F [fgCcell^{-1}d^{-1}ev]$$

206 Within the text, figures, equations and statistic results it is always referred to temperature corrected *in situ* bacterial
 207 production. Temperature corrected bacterial production and original bacterial production measured during incubation
 208 can be compared in supplementary Table 2.

209 The bacterial oxygen demand (BOD; $mmol O_2 m^{-3} d^{-1}$) is the amount of oxygen needed to fully oxygenize organic
 210 carbon that has been taken up and not transformed into biomass by bacterial production ($mmol C m^{-3} d^{-1}$). The BOD
 211 was calculated as the difference between the estimated bacterial DOC uptake and the bacterial production applying a
 212 respiratory quotient (cf) of 1 (Eq. (4)) (Del Giorgio and Cole, 1998).

213 4. $BOD = (DOC\ uptake - bacterial\ production) \times cf$

214 The bacterial DOC uptake was calculated under two different assumptions: i) the DOC uptake by bacteria equals the
 215 DOC loss rate over depth or ii) the bacterial growth efficiency (BGE) follows the established temperature
 216 dependence ($BGE = 0.374[\pm 0.04] - 0.0104[\pm 0.002]T [^{\circ}C]$), resulting in a BGE between 0.1 and 0.3 in the depth range
 217 of 10-60 m and an *in situ* temperature of 14 to 19°C (Rivkin and Legendre, 2001) and can be used to estimate the
 218 bacterial DOC uptake from bacterial production (Eq. (5)).

219 5. $bacterial\ DOC\ uptake = \frac{bacterial\ production}{BGE}$

220 2.6.Extracellular enzyme rates

221 Potential hydrolytic rates of LAPase and GLUCase were determined with fluorescent substrate analogues (Hoppe,
 222 1983). L-leucine-7-amido-4-methylcoumarin (Sigma Aldrich) and 4-methylumbelliferyl- β -D-glucopyranoside
 223 (Acros Organics) were added in final concentrations of 1, 5, 10, 20, 50, 80, 100 and 200 $\mu mol l^{-1}$ in black 69 well
 224 plates (Costar) and kept frozen for at most one day until replicates of 200 μl sample were added. After 0 and 12
 225 hours of incubation at 13°C in the dark, fluorescence was measured with a plate reader fluorometer (FLUOstar
 226 Optima, BMG labtech) (excitation: 355 nm; emission: 460 nm). An error of 2 % RSD was defined using the
 227 calibration with triplicates. Blanks with MilliQ were performed to exclude an increase in substrate decay over time.

228 Samples were collected in replicates ($n=2$) at station A-K and incubated directly after sampling under oxygen
 229 conditions resembling *in situ* oxygen conditions. For samples > 5 μmol *in situ* $O_2 kg^{-1}$ incubations were conducted
 230 under atmospheric oxygen conditions. Samples < 5 μmol *in situ* $O_2 kg^{-1}$ were incubated in a gas tight incubator that

231 had two openings to fill and flush it with gas. For our experiment the incubator was flushed and filled with N₂, to
 232 reduce oxygen concentrations. Still control measurements occasionally revealed oxygen concentrations of 8 to 40
 233 μmol O₂ kg⁻¹. Additionally, samples were in contact with oxygen during pipetting and measurement. To investigate
 234 the influence of the different incubation methods we additionally incubated samples > 5 μmol *in situ* O₂ kg⁻¹ under
 235 reduced oxygen concentrations. On average incubations under reduced oxygen concentration yielded 2-27% higher
 236 values than those incubated under atmospheric oxygen conditions. However, the observed trends over depth
 237 remained similar (see supplementary discussion).

238 Calibration was conducted with 7-amino-4-methylcoumarin (2 nmol l⁻¹ to 1 μmol l⁻¹) (Sigma Aldrich) and 4-
 239 methylumbelliferone (Sigma Aldrich) (16 nmol l⁻¹ to 1 μmol l⁻¹) in seawater at atmospheric oxygen concentrations
 240 and under N₂ atmosphere.

241 Maximum reaction velocity (V_{max}) at saturating substrate concentrations was calculated using both replicates at once,
 242 with the simple ligand binding function in SigmaPlot™ 12.0 (Systat Software Inc., San Jose, CA). Values for V_{max}
 243 with a SD >30 % were excluded from further analyses. The degradation rate (δ) [μmol C m⁻³ d⁻¹] of DHAA by
 244 LAPase and DCHO by GLUCase was calculated after Piontek et al. (2014):

$$245 \quad 6. \quad \delta = \frac{h_r * c}{100}$$

246 where h_r [% d⁻¹] is the hydrolyses turnover at 10³ μmol m⁻³ substrate concentration and c is the carbon content of
 247 DHAA [μmol C m⁻³]. Measurements of h_r with a SD between duplicates of more than 30% were excluded. The same
 248 procedure was conducted with the carbon content of dissolved hydrolysable leucine, instead of DHAA, to account
 249 for variations in leucine concentrations, which is the main amino acid hydrolysed by LAPase.

250 Similar to bacterial production, *in situ* extracellular enzyme rates were estimated based on extracellular enzyme rates
 251 measured during incubation. To account for the differences between *in situ* and incubation temperatures a correction
 252 factor (F) was applied based on differences in extracellular enzyme rates after additional incubations at 22.4°C next
 253 to the regular incubations at 13°C at five stations during the cruises. The fluorescence signals at different substrate
 254 concentrations increased on average by a factor of 0.05 and 0.03 (°C⁻¹) for GLUCase and LAPase, respectively.
 255 Under the assumption that the increase in rates with temperature was linear, measured enzyme rates were adapted to
 256 *in situ* temperature, with (EER_{insitu} ; nmol L⁻¹ h⁻¹) and ($EER_{incubation}$) being the *in situ* extracellular enzyme rates and
 257 extracellular enzyme rates during incubation, respectively:

$$258 \quad 7. \quad \delta T [^{\circ}C] = T_{insitu} [^{\circ}C] - T_{incubation} [^{\circ}C]$$

259

$$260 \quad 8. \quad EER_{insitu} [nmolL^{-1}h^{-1}] =$$

$$EER_{incubation} [nmolL^{-1}h^{-1}] + EER_{incubation} [nmolL^{-1}h^{-1}] \times F [^{\circ}C^{-1}] \times \delta T [^{\circ}C]$$

261 Within the text, figures, equations and statistic results it is always referred to the temperature corrected *in situ*
262 extracellular enzyme rates. Temperature corrected extracellular enzyme rates and original extracellular enzyme rates
263 measured during incubation can be compared in supplementary Table 2.

264 **2.7.Data analyses**

265 Data were plotted with Ocean Data View 4.74 (Schlitzer, 2016), MATLAB (8.3.0.532 (R2014a)) and R version 3.4.2
266 using the package *ggplot2* (Hadley Wickham, 2016; R Development Core Team, 2008). Statistical significances
267 between different regimes (see supplementary Table 2 for mean and SD within different regimes and statistical
268 results) were tested with a *Wilcoxon test* (W) and correlation with the *Spearman Rank correlation* (S) in R version
269 3.4.2 (R Development Core Team, 2008) using following R packages: *FSA*, *car* and *multcomp* (Derek H. Olge,
270 2018; Horthorn et al., 2008; John Fox and Sanford Weisberg, 2011). For this extracellular enzyme data of station A-
271 K and bacterial production data of station G-T were used, since not all parameters could be sampled at all depth.
272 Diapycnal fluxes of DOC and oxygen were calculated with MATLAB (8.3.0.532 (R2014a)) and the Toolbox Gibbs
273 SeaWater (GSW) Oceanographic Toolbox (3.05) (McDougall and Barker, 2011).

274 Samples were categorized into different oxygen regimes. Due to sensitivities of oxygen measurements, we did not
275 distinguish between anoxic and suboxic regimes, but defined the suboxic “OMZ” oxygen regime by a threshold ≤ 5
276 $\mu\text{mol O}_2 \text{ kg}^{-1}$ (Gruber, 2011). We defined the oxycline as one regime (>5 to $<60 \mu\text{mol O}_2 \text{ kg}^{-1}$) including the upper
277 and lower oxycline or separated it into “low_hypoxic” (>5 to $<20 \mu\text{mol O}_2 \text{ kg}^{-1}$) and “high_hypoxic” (>20 to <60
278 $\mu\text{mol O}_2 \text{ kg}^{-1}$) regimes, representing important thresholds of oxygen concentrations for biological processes (Gruber,
279 2011). Oxygen concentrations $>60 \mu\text{mol O}_2 \text{ kg}^{-1}$ were defined as “oxic”. Moreover, we partly differentiated between
280 oxygen regimes situated above and below the OMZ (see supplementary Table 2 for results).

281 **3. Results**

282 **3.1. Biogeochemistry of the Peruvian OMZ**

283 During our two cruises to the Peruvian upwelling system (Fig. 1), maximum Chl *a* concentration was higher and
284 temperatures were warmer in April compared to June 2017, probably representing seasonal variability. Chl *a*
285 concentration reached up to 11 and 4 $\mu\text{g l}^{-1}$ within the upper 25 m in April and June, respectively. Still, average Chl *a*
286 concentration at depth <10 m (M136: $3.1 \pm 2.6 \mu\text{g l}^{-1}$; M138: $2.8 \pm 1.3 \mu\text{g l}^{-1}$) were not significantly different between
287 the two cruises. At depths >50 m, Chl *a* concentration was generally below detection limit (Fig. 3a, supplementary
288 Fig. 1). At depth <10 m the water was warmer in April ($21.3 \pm 1.6^\circ\text{C}$) than in June ($17.6 \pm 0.6^\circ\text{C}$) (Fig. 3b,
289 supplementary Fig. 1). Oxygen concentration $>100 \mu\text{mol kg}^{-1}$ was observed in the surface mixed layer. Oxygen
290 decreased steeply with depth, reached suboxic concentrations ($<5 \mu\text{mol kg}^{-1}$) at $> 60 \pm 24$ m (Fig. 2c, 4a and 5a,
291 supplementary Fig.1) and fell below detection of Winkler titration. For further analysis and within the text *in situ*
292 oxygen concentrations $<5 \mu\text{mol O}_2 \text{ kg}^{-1}$ are referred to as “suboxic”. Shallowest depth with suboxic oxygen
293 concentrations was 14 m in April (station Q) and 29 m in June (station D), probably representing that station Q was
294 situated closer to the shore than station D. Oxygen increased again to up to 15 $\mu\text{mol kg}^{-1}$ at >500 m (Fig. 4a and 5a,

295 supplementary Fig. 1). TDN concentrations increased with depth from $18 \pm 8 \mu\text{mol l}^{-1}$ and $22 \pm 7 \mu\text{mol l}^{-1}$ within the
296 upper 20 m in April and June, respectively, and reached a maximum of $54 \mu\text{mol l}^{-1}$ at 850 m (Fig. 3c). DOC
297 decreased with depth from $94 \pm 37 \mu\text{mol l}^{-1}$ and $69 \pm 12 \mu\text{mol l}^{-1}$ in the upper 20 m in April and June, respectively, to
298 lowest values of $37 \mu\text{mol l}^{-1}$ at 850 m. The steepest gradient in DOC concentration was observed in the upper 20-60
299 m (Fig. 2b and 3d) during both cruises.

300 **3.2. Bacterial production and enzymatic activity**

301 Bacterial production varied strongly throughout the study region and ranged from 0.2 to $2404 \mu\text{mol C m}^{-3} \text{d}^{-1}$ (Fig.
302 4b), decreased in general from surface to depth (except for the most coastal station) and showed significantly higher
303 rates in the oxygenated surface compared to the OMZ (Fig. 4b). At the most coastal station (G) bacterial production
304 remained high near the bottom depth of 75 m ($280 \mu\text{mol C m}^{-3} \text{d}^{-1}$ at 72 m) (Fig. 4b). Bacterial production did not
305 differ significantly between the oxyclines and the suboxic core waters, neither off-shore (suboxic: $0.3\text{-}127 \mu\text{mol C m}^{-3} \text{d}^{-1}$;
306 oxyclines: $1\text{-}304 \mu\text{mol C m}^{-3} \text{d}^{-1}$) nor at the most coastal stations (G and T) (suboxic: $146\text{-}281 \mu\text{mol C m}^{-3} \text{d}^{-1}$)
307 (oxycline: $74\text{-}452 \mu\text{mol C m}^{-3} \text{d}^{-1}$) (see supplementary Table 2 for all statistical results). Further, no significant
308 correlation was observed between bacterial production and oxygen at *in situ* $<20 \mu\text{mol O}_2 \text{kg}^{-1}$. Additionally,
309 significantly lower bacterial production was observed within the lower oxycline ($0.7\text{-}3.3 \mu\text{mol C m}^{-3} \text{d}^{-1}$) compared
310 to the core OMZ ($0.3\text{-}281 \mu\text{mol C m}^{-3} \text{d}^{-1}$) even though oxygen increased from <5 to $15 \mu\text{mol kg}^{-1}$ (Fig. 4a, b).
311 Trends between oxygen regimes were similar between temperature corrected bacterial production (presented
312 throughout the text) and original bacterial production measured during incubation (supplementary Table 2).

313 Overall, bacterial abundance ranged from 1 to $49 \times 10^5 \text{ cells ml}^{-1}$, with highest abundance observed at the surface and
314 close to the sediment. Cell abundance in the oxyclines ($1\text{-}16 \times 10^5 \text{ cells ml}^{-1}$) was significantly lower than in the
315 OMZ core ($1\text{-}25 \times 10^5 \text{ cells ml}^{-1}$) (Fig. 4c). A sharp decrease in bacterial abundance was observed below the OMZ.

316 Estimates for the *in situ* degradation rate of DHAA by LAPase take into account the available concentrations of
317 DHAA and varied between 0.7 and $39.7 \mu\text{mol C m}^{-3} \text{d}^{-1}$. LAPase degradation rates observed within the OMZ core
318 ($5.5 \pm 2.1 \mu\text{mol C m}^{-3} \text{d}^{-1}$) were significantly higher than in the oxyclines ($3.1 \pm 2.3 \mu\text{mol C m}^{-3} \text{d}^{-1}$) (Fig. 5b). To
319 exclude an influence of changing DHAA composition over depth, LAPase activity was also calculated using *in situ*
320 concentrations of dissolved hydrolysable leucine instead of total DHAA. Degradation rates of dissolved hydrolysable
321 leucine by LAPase ($0.01\text{-}1.92 \mu\text{mol C m}^{-3} \text{d}^{-1}$) showed the same trend with significantly higher rates in suboxic
322 waters than in the oxyclines. Thus, differences in the molecular composition of DHAA had no influence on spatial
323 degradation patterns being higher in suboxic waters than in the upper oxycline. In contrast, degradation rates of
324 DCHO ($>1\text{kDa}$) were slightly reduced within the suboxic waters ($0.69 \pm 1.30 \mu\text{mol C m}^{-3} \text{d}^{-1}$) compared to the
325 oxyclines ($1.1 \pm 1.0 \mu\text{mol C m}^{-3} \text{d}^{-1}$) (Fig. 5c). Since degradation rates were calculated by multiplying enzyme rates
326 and carbon concentrations of DCHO and DHAA at *in situ* depth, differences in carbon concentrations are important
327 for further interpretation. *In situ* carbon concentrations of DHAA were similar between the OMZ core (0.53 ± 0.1
328 $\mu\text{mol C L}^{-1}$) and the oxycline ($0.57 \pm 0.2 \mu\text{mol C L}^{-1}$). In contrast, *in situ* carbon concentrations of DCHO were
329 reduced within the OMZ core ($1.3 \pm 0.4 \mu\text{mol C L}^{-1}$) compared to the oxycline ($1.5 \pm 0.6 \mu\text{mol C L}^{-1}$) (Fig. 3e, f),
330 suggesting that calculated differences between degradation rates may be influenced by different carbon

331 concentrations. Potential hydrolytic rates at saturating substrate concentration (V_{\max}) of LAPase ranged between 9
332 and 158 $\text{nmol l}^{-1} \text{h}^{-1}$ and were ~ 30 times lower for GLUCase. LAPase V_{\max} was significantly higher within the
333 suboxic waters ($50 \pm 21 \text{ nmol l}^{-1} \text{h}^{-1}$) compared to the oxycline ($36 \pm 20 \text{ nmol l}^{-1} \text{h}^{-1}$) and GLUCase V_{\max} was more
334 similar within the suboxic waters ($1.6 \pm 1.5 \text{ nmol l}^{-1} \text{h}^{-1}$) compared to the oxycline ($1.2 \pm 0.6 \text{ nmol l}^{-1} \text{h}^{-1}$) (Fig. 5d, e).
335 Trends between oxygen regimes were similar between temperature corrected extracellular enzyme rates (presented
336 throughout the text) and extracellular enzyme rates measured during incubation (supplementary Table 2).

337 To investigate physiological effects of suboxia, we normalized bacterial production and enzymatic rates to cell
338 abundance. Cell-specific production ranged between 1 and 1120 $\text{amol C cell}^{-1} \text{d}^{-1}$ (Fig. 4d). In contrast to total
339 production, cell-specific production was significantly higher at the oxyclines compared to suboxic core waters at the
340 off-shore stations (suboxic: $1\text{-}102 \mu\text{mol C m}^{-3} \text{d}^{-1}$, oxyclines: $6\text{-}219 \mu\text{mol C m}^{-3} \text{d}^{-1}$). At the most coastal stations (G
341 and T) cell-specific rates were more similar between suboxic waters and the oxyclines (suboxic: $129\text{-}135 \mu\text{mol C m}^{-3}$
342 d^{-1}) (oxycline: $72\text{-}284 \mu\text{mol C m}^{-3} \text{d}^{-1}$). Further, cell-specific bacterial production was slightly correlated (spearman
343 rank correlation =0.36) to oxygen concentrations at $\leq 20 \mu\text{mol O}_2 \text{ kg}^{-1}$ and as long as the most coastal stations (G and
344 T) were included this correlation was significant (Fig. 4d, supplementary Table 2). A detailed view at total- and cell-
345 specific bacterial production in dependence of *in-situ* oxygen concentrations, reveals a stronger increase of cell-
346 specific bacterial production, especially at $< 10 \mu\text{mol O}_2 \text{ kg}^{-1}$ at different stations (supplementary Fig. 2).

347 Cell-specific degradation rates of DHAA increased with depth and yielded significantly higher rates at the lower
348 oxycline compared to all shallower depths. Cell-specific LAPase V_{\max} , GLUCase V_{\max} and GLUCase degradation
349 rate showed the same trends, however for the latter this trend was not significant (Fig. 5g-j, supplementary Table 2)

350 **3.3.Bacterial contribution to the loss of dissolved organic carbon and oxygen in the** 351 **oxycline**

352 We calculated the loss of oxygen and DOC during physical transport from below the mixed layer depth (MLD; 10-
353 32 m) to 60 m based on observed changes in diapycnal fluxes (Eq. (1), Fig. 2b, c). We estimated the bacterial
354 contribution to this loss using two different approaches (Table 1): i) We assumed that the loss of DOC over depth
355 equalled the bacterial uptake implying that the DOC is subsequently incorporated as bacterial biomass (bacterial
356 production) or respired to CO_2 (Eq. (4)) ii) the amount of DOC taken up by bacteria was determined by the measured
357 bacterial incorporation of carbon (bacterial production) and a constant ratio between carbon that is taken up and
358 carbon that is incorporated as biomass (bacterial production) (Eq. (5)) (see section 2.5 for details). This ratio (BGE),
359 was here assumed to be 10 or 30%, based on the empirical equation by Rivkin and Legendre with an *in situ*
360 temperature that varied between 14 and 19°C (Rivkin and Legendre, 2001).

361 For total average DOC loss ($\nabla\Phi_{\text{DOC}}$), we calculated a range of $1.13\text{-}3.40 \text{ mmol C m}^{-3} \text{d}^{-1}$, with loss rates decreasing
362 most strongly below the shallow mixed layer down to 40 m (Table 1, Fig. 2c). Following the first (i) assumption, all
363 DOC that was lost over depth was taken up by bacteria and the measured bacterial production represents the fraction
364 of DOC that was incorporated as biomass. Consequently, the remaining DOC that has been taken up, in other words
365 the difference between DOC loss and bacterial production ($0.03\text{-}0.71 \text{ mmol C m}^{-3} \text{d}^{-1}$), was respired to CO_2 and

366 represents the bacterial oxygen demand to account for the DOC loss (BOD_g) ($0.98-3.36 \text{ mmol O}_2 \text{ m}^{-3} \text{ d}^{-1}$) (Eq. (4)).
367 Following this calculation, the BGE would vary between 1-21 % and 2 -13 % in the depth range of MLD-40 m and
368 40-60 m, respectively, being on average almost constant over the two different depth ranges (6.6 and 5.0%). ii)
369 Applying a BGE in the range of 10 and 30% and the measured bacterial production, the calculated bacterial DOC
370 uptake ϕ was $0.08-7.10 \text{ mmol C m}^{-3} \text{ d}^{-1}$. Hence, respiration of DOC to CO_2 accounted for a BOD_ϕ of $0.06-6.39 \text{ mmol}$
371 $\text{O}_2 \text{ m}^{-3} \text{ d}^{-1}$ (Table 1).

372 4. Discussion

373 We investigated bacterial degradation of DOM by measuring bacterial production as an estimate for organic carbon
374 transformation into biomass as well as rates of extracellular hydrolytic enzymes to provide information on the initial
375 steps of organic matter degradation (Hoppe et al., 2002). We expected reduced rates of organic matter degradation
376 within oxygen depleted waters, since reduced bacterial degradation activity might explain enhanced carbon fluxes in
377 suboxic and anoxic waters (Devol and Hartnett, 2001). However, although bacterial production decreased with depth
378 (Fig. 4b), this decrease was not related to oxygen concentrations. Moreover, no significant increase in bacterial
379 production was observed at the lower oxycline, when oxygen concentration increased again (Fig. 4b). Decreasing
380 bacterial production with depth has also been observed for fully oxygenated regions in the Atlantic (Baltar et al.,
381 2009) and the equatorial Pacific (Kirchman et al., 1995) and has been explained by a decrease in the amount of
382 bioavailable organic matter over depth.

383 The hypothesis of reduced bacterial degradation activity within the OMZ also implies reduced extracellular enzyme
384 rates for the hydrolysis of organic matter. The extracellular enzymes rates of our study have to be interpreted
385 carefully since incubation was not fully anoxic and the remaining oxygen might have biased the results. Still, we
386 assume that most extracellular enzymes were present at the time of sampling and thus oxygen contamination during
387 the incubations did not strongly influence the rate measurements. In our study, neither GLUCase nor LAPase V_{\max}
388 were reduced within the suboxic waters compared to the oxyclines irrespective of incubation conditions (Fig. 5d, e,
389 supplementary Fig. 3 and 4). Thus, our findings show no evidence for reduced organic matter degradation in suboxic
390 waters and are in good agreement with studies, which report similar bacterial degradation rates for oxic and suboxic
391 waters (Cavan et al., 2017; Lee, 1992; Pantoja et al., 2009). Consequently, the hypothesis of enhanced carbon export
392 in OMZ waters due to reduced organic matter degradation seems fragile and alternative explanations for enhanced
393 carbon export efficiency e.g. reduced particle fragmentation due to zooplankton avoiding hypoxia (Cavan et al.,
394 2017) may be more likely. Likewise, a reduced degradation of particulate organic carbon in suboxic waters as it is
395 often assumed in global ocean biogeochemical models may have to be reconsidered (Ilyina et al., 2013).

396 Within OMZs dissolved nitrogen fuels e.g. denitrification or anaerobic ammonium oxidation (anammox) and is
397 reduced to e.g. dinitrogen gas that evades to the atmosphere. Current estimates result in 20-50% of the total oceanic
398 nitrogen loss occurring in OMZs (Lam and Kuypers, 2011). Meanwhile, a preferential degradation of amino acid
399 containing organic matter in suboxic waters compared to oxic waters has been suggested (Van Mooy et al., 2002).

400 Degradation of nitrogen compounds by heterotrophic bacteria (e.g. denitrifiers) in suboxic waters enables the release
401 of ammonia and nitrite and subsequently may support anammox, an autotrophic anaerobic pathway (Babbin et al.,
402 2014; Kalvelage et al., 2013; Lam and Kuypers, 2011; Ward, 2013). This interaction between denitrifiers and
403 anammox bacteria could fuel the loss of nitrogen to the atmosphere. Our data indeed showed enhanced degradation
404 of amino-acid-containing organic matter in low oxygen waters. Indicators for protein decomposition, i.e. LAPase
405 V_{max} and the degradation rate of DHAA by LAPase, were more pronounced within the suboxic waters (Fig. 5b, d).
406 Therefore, observed LAPase rates are in line with the hypothesis of preferential degradation of nitrogen compounds
407 under suboxia. However, simultaneous rate measurements of protein hydrolysis, nitrate reduction (e.g.
408 denitrification) and anammox are needed to prove an indirect stimulation of anammox by protein hydrolysis via
409 denitrification. A close coupling between anammox and nitrate reducing bacteria has previously been shown for
410 wastewater treatments. There, nitrate reducers directly take up organic matter excreted by the anammox bacteria
411 which in turn benefit from the released nitrite by respiratory nitrate reduction (Lawson et al., 2017). In the Pacific,
412 denitrifiers and anammox bacteria are separated in space and time (Dalsgaard et al., 2012), potentially weakening a
413 direct inter-dependency.

414 To investigate physiological effects of suboxia, we normalized bacterial production and enzymatic rates to cell
415 abundance and found higher cell-specific bacterial production near the oxycline compared to suboxic waters and
416 highest cell-specific enzyme rates at the lower oxycline (Fig. 4d, 5g-j). Higher cell-specific bacterial production at
417 oxic-anoxic interfaces in the water column has previously been reported for the Baltic Sea (Brettar et al., 2012).
418 Baltar et al. (2009) showed increasing cell-specific enzymatic rates and decreasing cell-specific bacterial production,
419 with increasing depth in the subtropical Atlantic and related this pattern to decreasing organic matter lability. In our
420 study, differences in cell-specific bacterial production between suboxic waters and the oxycline did not persist at the
421 most coastal stations (G and T). This indicates the stimulation of bacterial activity, including anaerobic respiratory
422 processes, by the high input of labile organic matter. Therefore, our study suggests that a possible impairment of cell-
423 specific bacterial production under suboxia is reduced by supply of organic matter. However, this hypothesis is
424 restricted to a very limited number of samples and should be tested in further studies. While labile organic matter is
425 decreasing with depth (e.g. Loginova et al., 2019), TDN (Fig. 3c), especially inorganic nitrogen is increasing with
426 depth. Thus, high concentrations of inorganic nitrogen at the lower oxycline are available for heterotrophic and
427 chemoautotrophic energy gains. For instance, the co-occurrence of nitrate reduction, that was still detected at 25
428 $\mu\text{mol O}_2 \text{ L}^{-1}$, and microaerobic respiration might have stimulated cell-specific production or the accumulation of
429 especially active bacterial species (Kalvelage et al., 2011, 2015).

430 Depth distribution of cell-specific and total bacterial production was different (Fig. 4b, d and supplementary Fig. 2);
431 cell-specific production was significantly reduced in suboxic waters, while total production was more similar in
432 suboxic waters compared to the oxycline. This suggests that lower cell-specific production was compensated by
433 higher cell abundance within the suboxic waters (Fig. 4c), resulting in an overall unhampered bacterial organic
434 matter cycling in the OMZ core. One reason for the accumulation of cells within the OMZ might be reduced
435 predation, suggesting the OMZ core as an ecological niche for slowly growing bacteria. Reduced grazing by
436 bacterivores thus preserves bacterial biomass in suboxic waters from entering into the food chain. This way of

437 bacterial biomass preservation has been suggested as possible explanation for enhanced carbon preservation in
438 anoxic sediments by Lee (1992), and may also explain our observations for the anoxic water column.

439 In general, bacterial community composition in OMZs has been shown to be strongly impacted by oxygen. In the
440 OMZ near the shelf off Chile Arctic96BD-19 and SUP05 dominate heterotrophic and autotrophic groups in hypoxic
441 waters (Aldunate et al., 2018). Next to the appearance of autotrophic bacteria that are related to sulphur (e.g. SUP05)
442 or nitrogen cycling (e.g. Planctomycetes), also bacteria related to cycling of complex carbohydrates have been
443 discovered in OMZs (Callbeck et al., 2018; Galán et al., 2009; Thrash et al., 2017), and may explain the unaltered
444 high potential (V_{max}) of the extracellular enzymes GLUCase and heterotrophic bacterial production in suboxic waters
445 in our study (Fig. 5e, 4b). For instance, SAR406, SAR202, ACD39 and PAUC34f have the genetic potential for the
446 turnover of complex carbohydrates and anaerobic respiratory processes, in the Gulf of Mexico (Thrash et al., 2017).
447 Consequently, our findings of active bacterial degradation of DOM are supported by molecular biological studies.
448 Still, simultaneous measurements of bacterial degradation and production have to be combined with molecular
449 analysis, in future studies off Peru.

450 Heterotrophic bacteria are the main users of marine DOM (Azam et al., 1983; Carlson and Hansell, 2015) and
451 responsible for ~79% of total respiration in the Pacific Ocean (Del Giorgio et al., 2011), proposing that heterotrophic
452 bacteria drive organic matter and oxygen cycling in the ocean and significantly contribute to the formation of the
453 OMZ. Under the assumption that the calculated loss of DOC during diapycnal transport (<60 m) is caused solely by
454 bacterial uptake and subtracting the amount of carbon channelled into biomass production, our study verifies the
455 importance of bacterial DOC degradation for the formation of the OMZ. We estimated a BOD ($0.98-3.36 \text{ mmol O}_2$
456 $\text{m}^{-3} \text{ d}^{-1}$) that is in line with earlier respiration measurements in the upper oxycline off Peru (Kalvelage et al., 2015)
457 and represents 18-33% of the oxygen loss over depth, implying a rather low average BGE (6.5 and 5.0 %) (Table 1).
458 Calculating the bacterial uptake of DOC from production rates and a more conservative BGE between 10 and 30% as
459 previously suggested (Rivkin and Legendre, 2001) for the *in situ* temperature of 14 to 19 °C, 3-209% of the DOC
460 loss and 1-62% of oxygen loss could be attributed to bacterial degradation of DOM. The first approach reveals an
461 average BGE (6.5 and 5.0%) that is still within the range of previous reports for upwelling systems of the Atlantic
462 (<1-58%) and northeastern Pacific (<10%) (Alonso-Sáez et al., 2007; Del Giorgio et al., 2011). The high variability
463 in BGE is a topic of ongoing research. Until now 54% of the variability could be explained by variations in
464 temperature (Rivkin and Legendre, 2001). Our data suggest that oxygen availability may be another control of BGE
465 leading to rather low BGE in low oxygen waters. This is especially indicated by a low but rather constant average
466 BGE (6.5 and 5.0%), which we estimated for the water column down to 60_m depth under the assumption that all
467 DOC that is lost over depth can be attributed to bacterial uptake. A low BGE might be explained by a bacterial
468 community that has higher energetic demands, but in return is adapted to variable oxygen conditions. Additionally,
469 the BGE is decreasing with an increasing carbon to nitrogen ratio of the available substrate (Goldman et al., 1987).
470 In the OMZ off Peru the ratio between DOC and dissolved organic nitrogen is frequently high (~12 to 16) (Loginova
471 et al., 2019), and might further contribute to the low BGE. High respiration rates induced by bacterial DOC
472 degradation contribute to sustaining the OMZ, besides oxygen consumption by bacteria that hydrolyze and degrade
473 particulate organic matter (Cavan et al., 2017). Another, but likely minor contribution to overall respiration is made

474 by zooplankton and higher trophic levels (e.g. Kiko et al., 2016). Additionally, physical processes such as an
475 intrusion of oxygen depleted waters by eddies, upwelling or advection, may add to the oxygen and DOC loss over
476 depth (Brandt et al., 2015; Llanillo et al., 2018; Steinfeldt et al., 2015).

477 Uncertainties of our assumption that the loss of DOC is caused solely by bacterial uptake include other processes
478 potentially contributing to DOC removal, but not taken into consideration here like DOC adsorption onto particles,
479 DOC uptake by eukaryotic cells or the physical coagulation of DOC into particles, e.g. by formation of gel-like
480 particles such as transparent exopolymer particles and Coomassie stainable particles (Carlson and Hansell, 2015;
481 Engel et al., 2004, 2005). Moreover, temporal variations in diapycnal fluxes may be large, as indicated by the
482 confidence interval of solute fluxes (Fig. 2b, c) during this study and by 2 to 10 times lower DOC and oxygen loss
483 rates during other seasons (Loginova et al., 2019). However, our study is the first combining physical and microbial
484 rate measurements and gives estimates for carbon and oxygen losses in the upwelling system off Peru and can help
485 improving current biogeochemical models by constraining bacterial DOM degradation.

486 Loginova et al. (2019) conducted similar physical rate measurements in the same study area with ~2 and ~10 times
487 lower DOC and oxygen loss in the upper ~40 m compared to our study. Differences in loss rates were mainly caused
488 by a ~ 10 times higher diapycnal diffusivity of mass in our study. This may have been caused by weaker
489 stratification in the upper 100 m depth or differences in the turbulence conditions. Loginova et al. (2019) estimated a
490 contribution of bacterial DOM degradation to oxygen loss (38 %) based on the loss of labile DOC (DHAA and
491 DCHO). This value agrees well with our estimates of 18-33% of total oxygen loss, calculated under the assumption
492 that DOC loss is solely attributed to bacterial degradation. However, the comparison of DOC and oxygen loss within
493 each study revealed different patterns. Loginova et al. (2019) found a loss of DOC that clearly exceeded the loss of
494 oxygen within the upper ~40 m. Hence, respiration of DOC could fully explain the observed oxygen loss in that
495 study. In our study, more oxygen than DOC was lost over depth (Table 1). This loss of oxygen needs additional
496 explanations such as degradation of particulate organic matter and physical mixing processes. One reason for the
497 observed differences between the two studies that have been conducted in the same region might be seasonality. The
498 study by Loginova et al. (2019) took place in austral summer, whereas our data were gained during austral winter.
499 Water temperature was quite similar during both studies, probably due to the coastal El Niño one month before our
500 sampling campaign (Garreaud, 2018). Still, the study by Loginova et al. (2019) included more stations with high Chl
501 *a* concentrations (~8 µg L⁻¹), as typical for the austral summer, indicating a more productive system with more labile
502 DOM (DCHO and DHAA). Prevalence of more labile DOM might explain the higher contribution of microbial
503 DOM respiration to oxygen loss in the study by Loginova et al. (2019). ~~Additionally, Loginova et al. (2019) sampled
504 with a much higher vertical resolution within the upper 140 m, restricting the direct comparability with our study.~~

506 In oxygen depleted waters of the Peruvian upwelling system, the chemoautotrophic process of anammox has been
507 assumed to dominate anaerobic nitrogen cycling (Kavelage et al., 2013), with lower but more constant rates
508 compared to more sporadically occurring heterotrophic denitrification (Dalsgaard et al., 2012). Studies based on the
509 stoichiometry of organic matter suggest a general dominance of denitrification in relation to anammox and relate
510 variable ratios between these two processes to the stoichiometry of locally available organic matter (Babbin et al.,

511 | 2014; Ward, 2013). Our study points towards a widespread occurrence of heterotrophic anaerobic denitrification
512 | processes such as denitrification or sulfate reduction (Canfield et al., 2010) in the Peruvian OMZ, since the here
513 | applied method for measuring bacterial production is restricted to heterotrophs. Our rates for bacterial production
514 | within the suboxic waters averaged to $37 \mu\text{mol C m}^{-3} \text{ d}^{-1}$ ($0.3\text{-}281 \mu\text{mol C m}^{-3} \text{ d}^{-1}$).
515 |

516 | We compared bacterial production, i.e. rates of carbon incorporation, with denitrification rates previously reported
517 | for the South Pacific. Therefore, we converted one mol of reduced nitrogen that were measured by Dalsgaard et al.
518 | (2012) and Kalvelage et al. (2013) to 1.25 mol of oxidized carbon after the reaction equation given by Lam and
519 | Kuypers (2011). This calculation indicates that on average $\leq 19 \mu\text{mol C m}^{-3} \text{ d}^{-1}$ are oxidized by denitrifying bacteria
520 | in the Eastern Tropical Pacific (Dalsgaard et al., 2012; Kalvelage et al., 2013).

521 | The amount of carbon oxidized by denitrification based on the studies of Dalsgaard et al. (2012) and Kalvelage et al.
522 | (2013) can be converted into bacterial production applying a BGE. The average temperature dependent BGE was
523 | 20%. A BGE of 20% agrees well with other studies (Del Giorgio and Cole, 1998). Assuming a BGE of 20%, the
524 | denitrification rates of Dalsgaard et al. (2012) and Kalvelage et al. (2013) suggest a bacterial production of $\leq 5 \mu\text{mol}$
525 | $\text{C m}^{-3} \text{ d}^{-1}$, equivalent to only about 14% of total average heterotrophic bacterial production in suboxic waters
526 | determined in our study. For the sum of anaerobic carbon oxidation rates including denitrification, DNRA and
527 | simple nitrate reduction, $109 \mu\text{mol C m}^{-3} \text{ d}^{-1}$ ($6\text{-}515 \mu\text{mol C m}^{-3} \text{ d}^{-1}$) may be expected for the Peruvian shelf, with the
528 | reduction of nitrate to nitrite representing the largest proportion ($2\text{-}505 \mu\text{mol C}^{-1} \text{ m}^{-3} \text{ d}^{-1}$), based on the relative
529 | abundance of the different N-functional genes (Kalvelage et al., 2013). These anaerobic respiration measurements
530 | are equivalent to a bacterial production of $\sim 27 \mu\text{mol C m}^{-3} \text{ d}^{-1}$ ($1\text{-}129 \mu\text{mol C m}^{-3} \text{ d}^{-1}$) and are thus lower than our
531 | direct measurements of bacterial production rates. Moreover, the reduction of nitrate, could not be detected at every
532 | depth and incubation experiments partly showed huge variations over depth (Kalvelage et al., 2013), whereas we
533 | were able to measure bacterial production in every sample. The same calculation can be repeated assuming a BGE of
534 | 6%, which is the average BGE within this study based on DOC loss and bacterial production. Assuming a BGE of
535 | 6%, the estimated $109 \mu\text{mol C m}^{-3} \text{ d}^{-1}$ that are respired by anaerobic carbon oxidation (Kalvelage et al., 2013) would
536 | represent 94% of the carbon uptake. Consequently, $7 \mu\text{mol C m}^{-3} \text{ d}^{-1}$, i.e. 6% of the carbon uptake, are incorporated
537 | into the bacterial biomass. A bacterial biomass production of $7 \mu\text{mol C m}^{-3} \text{ d}^{-1}$ is even lower than the bacterial
538 | production of $27 \mu\text{mol C m}^{-3} \text{ d}^{-1}$, based on a BGE of 20% and cannot explain the average bacterial production
539 | measured in suboxic waters during our study ($37 \mu\text{mol C m}^{-3} \text{ d}^{-1}$). Therefore, this estimation suggests higher rates of
540 | heterotrophic anaerobic respiratory processes than previously measured. Since denitrification rates were not
541 | measured directly, the comparability of published denitrification rates and our measurements of bacterial production
542 | are limited. However, our data suggest that the carbon oxidation potential off Peru is more evenly horizontally and
543 | vertically distributed than expected and also corroborate earlier suggestions of unexpectedly high rates of
544 | heterotrophic nitrogen cycling in the OMZ off Peru based on observations of high concentrations of atmospheric
545 | nitrous oxide (Bourbonnais et al., 2017).

546 **5. Conclusion**

547 Our study suggests that suboxia does not reduce bacterial degradation of organic matter in the Eastern Tropical South
548 Pacific off Peru. Bacterial species are seemingly adapted to these environments and higher cell abundance
549 compensates for hampered cell-specific bacterial production under suboxia. Therefore, the previously observed
550 enhanced carbon export in OMZs compared to oxygenated waters requires alternative explanations. Differences
551 between cell-specific and total rates of bacterial activity allude to different controls of cell abundance in suboxic
552 systems, highlighting the OMZ as a specific ecological niche. The combination of bacterial and physical rate
553 measurements suggests that low BGEs in the upper oxycline contribute to sustaining the OMZ. Meanwhile, new
554 findings during our study call for additional studies: i) DOC loss differed strongly between our investigation and the
555 study of Loginova et al. (2019). Therefore, combined physical and biological rate measurements in the Peruvian
556 upwelling system should be repeated during austral summer, to learn more about the interplay of DOC loss and
557 bacterial production during different seasons. ii) Integrated measurements of denitrification, microaerobic respiration
558 and bacterial production are needed to estimate the fractions of incorporated and respired carbon under suboxia. The
559 BGE received in that way could support or disprove the low BGE estimate, which was calculated from DOC loss and
560 bacterial production in our study. Consequently, our study highlights the need for a better mechanistic understanding
561 and quantification of processes responsible for oxygen and DOM loss in OMZs that is inevitable to predict future
562 patterns of deoxygenation in a warming climate.

563 *Data Availability.* PANGAEA: 10.1594/PANGAEA.891247

564
565 *Author contributions.* M.M. and A.E. designed the scientific study, analysed the data and wrote the manuscript. J.L.
566 calculated DOC and oxygen fluxes, G.K. sampled and calibrated the CTD data and both J.L. and G.K. commented
567 on the manuscript.

568 *Competing interests.* The authors declare that they have no conflict of interest.

569 *Acknowledgments:* We thank Jon Roa, Tania Klüver and Ruth Flerus for the sampling and/or analysis of DOC/TDN;
570 cell abundance, bacterial production and DHAA. Moreover, we would like to thank Judith Piontek, Sören Thomsen,
571 Carolina Cisternas-Novoa and Frédéric A.C. Le Moigne who helped and gave advice for sampling during the cruises.
572 We are grateful to the working group of Hermann Bange and Stefan Sommer who provided Winkler measurements.
573 We thank the cruise leaders Hermann Bange and Marcus Dengler, crew, officers and the captains of the F.S. Meteor
574 for the support on board and the successful cruises. This study was supported by the Helmholtz Association and by
575 the Collaborative Research Center 754 / SFB Sonderforschungsbereich 754 'Climate-Biogeochemistry Interactions
576 in the Tropical Ocean'.

577 **References**

- 578 Aldunate, M., De la Iglesia, R., Bertagnolli, A. D. and Ulloa, O.: Oxygen modulates bacterial community
579 composition in the coastal upwelling waters off central Chile, *Deep. Res. Part II*, in press, 1–12,
580 doi:10.1016/j.dsr2.2018.02.001, 2018.
- 581 Alonso-Sáez, L., Gasol, J. M., Arístegui, J., Vilas, J. C., Vaqué, D., Duarte, C. M. and Agustí, S.: Large-scale
582 variability in surface bacterial carbon demand and growth efficiency in the subtropical northeast Atlantic Ocean,
583 *Limnol. Oceanogr.*, 52(2), 533–546, doi:10.4319/lo.2007.52.2.0533, 2007.
- 584 Azam, F., Fenchel, T., Field, J. G., Gray, J. S., Meyer-Reil, L. A. and Thingstad, F.: The ecological role of water-
585 column microbes in the sea., *Mar. Ecol. Prog. Ser.*, 10(3), 257–263, 1983.
- 586 Babbin, A. R., Keil, R. G., Devol, A. H. and Ward, B. B.: Organic matter stoichiometry, flux, and oxygen control
587 nitrogen loss in the ocean, *Science* ., 344(406), 406–408, doi:10.1126/science.1248364, 2014.
- 588 Bakund, A. and Nelson, C. S.: The seasonal cycle of wind-stress curl in subtropical eastern boundary current
589 regions., *J. Phys. Oceanogr.*, 21, 1815–1834, 1991.
- 590 Baltar, F., Arístegui, J., Sintès, E., van Aken, H. M., Gasol, J. M. and Herndl, G. J.: Prokaryotic extracellular
591 enzymatic activity in relation to biomass production and respiration in the meso- and bathypelagic waters of the
592 (sub)tropical Atlantic, *Environ. Microbiol.*, 11(8), 1998–2014, doi:10.1111/j.1462-2920.2009.01922.x, 2009.
- 593 Benner, R. and Amon, R. M. W.: The size-reactivity continuum of major bioelements in the ocean, *Ann. Rev. Mar.*
594 *Sci.*, 7(1), 185–205, doi:10.1146/annurev-marine-010213-135126, 2015.
- 595 Boetius, A. and Lochte, K.: Effect of organic enrichments on hydrolytic potentials and growth of bacteria in deep-sea
596 sediments., *Mar. Ecol. Prog. Ser.*, 140, 239–250, doi:10.3354/meps140239, 1996.
- 597 Bourbonnais, A., Letscher, R. T., Bange, H. W., Échevin, V., Larkum, J., Mohn, J., Yoshida, N. and Altabet, M. A.:
598 N₂O production and consumption from stable isotopic and concentration data in the Peruvian coastal upwelling
599 system, *Global Biogeochem. Cycles*, 31(4), 678–698, doi:10.1002/2016GB005567, 2017.
- 600 Brandt, P., Bange, H. W., Banyte, D., Dengler, M., Didwischus, S., Fischer, T., Greatbatch, R. J., Hahn, J., Kanzow,
601 T., Karstensen, J., Körtzinger, A., Krahnemann, G., Schmidtke, S., Stramma, L., Tanhua, T. and Visbeck, M.: On the
602 role of circulation and mixing in the ventilation of oxygen minimum zones with a focus on the eastern tropical North
603 Atlantic, *Biogeoscience*, 12, 489–512, doi:10.5194/bg-12-489-2015, 2015.
- 604 Brettar, I., Christen, R. and Höfle, M. G.: Analysis of bacterial core communities in the central Baltic by comparative
605 RNA–DNA-based fingerprinting provides links to structure–function relationships., *ISME J.*, 6(1), 195–212,
606 doi:10.1038/ismej.2011.80, 2012.
- 607 Callbeck, C. M., Lavik, G., Ferdelman, T. G., Fuchs, B., Gruber-Vodicka, H. R., Hach, P. F., Littmann, S.,

608 Schoffelen, N. J., Kalvelage, T., Thomsen, S., Schunck, H., Löscher, C. R., Schmitz, R. A. and Kuypers, M. M. M.:
609 Oxygen minimum zone cryptic sulfur cycling sustained by offshore transport of key sulfur oxidizing bacteria, *Nat.*
610 *Commun.*, 9(1729), 1–11, doi:10.1038/s41467-018-04041-x, 2018.

611 Canfield, D. E., Stewart, F. J., Thamdrup, B., Brabandere, L. De, Dalsgaard, T., Delong, E. F., Revsbech, N. P. and
612 Ulloa, O.: A Cryptic Sulfur Cycle in Oxygen-Minimum-Zone Waters off the Chilean Coast, *Science.*, 330, 1375–
613 1379, doi:10.1126/science.1196889, 2010.

614 Carlson, C. A. and Hansell, D. A.: DOM sources, sinks, reactivity, and budgets, in *Biogeochemistry of marine*
615 *dissolved organic matter*, edited by C. A. Carlson and D. A. Hansell, pp. 65–126, Elsevier, London., 2015.

616 Cavan, E. L., Trimmer, M., Shelley, F. and Sanders, R.: Remineralization of particulate organic carbon in an ocean
617 oxygen minimum zone, *Nat. Commun.*, 8, doi:10.1038/ncomms14847, 2017.

618 Cole, J. J. and Pace, M. L.: Bacterial secondary production in oxic and anoxic freshwaters, *Limnol. Oceanogr.*, 40(6),
619 1019–1027, doi:10.4319/lo.1995.40.6.1019, 1995.

620 Czeschel, R., Stramma, L., Schwarzkopf, F. U., Giese, B. S., Funk, A. and Karstensen, J.: Middepth circulation of
621 the eastern tropical South Pacific and its link to the oxygen minimum zone, *J. Geophys. Res.*, 116(C01015), 1–13,
622 doi:10.1029/2010JC006565, 2011.

623 Dalsgaard, T., Thamdrup, B., Farías, L. and Revsbech, N. P.: Anammox and denitrification in the oxygen minimum
624 zone of the eastern South Pacific, *Limnol. Oceanogr.*, 57(5), 1331–1346, doi:10.4319/lo.2012.57.5.1331, 2012.

625 Del Giorgio, P. A. and Cole, J. J.: Bacterial growth efficiency in natural aquatic systems, *Annu. Rev. Ecol. Syst.*, 29,
626 503–541, 1998.

627 Del Giorgio, P. A., Condon, R., Bouvier, T., Longnecker, K., Bouvier, C., Sherr, E. and Gasol, J. M.: Coherent
628 patterns in bacterial growth, growth efficiency, and leucine metabolism along a northeastern Pacific inshore-offshore
629 transect, *Limnol. Oceanogr.*, 56(1), 1–16, doi:10.4319/lo.2011.56.1.0001, 2011.

630 Derek H. Olge: FSA: Fisheries Stock Analysis, 2018.

631 Devol, A. H. and Hartnett, H. E.: Role of the oxygen-deficient zone in transfer of organic carbon to the deep ocean,
632 *Limnol. Oceanogr.*, 46(7), 1684–1690, doi:10.4319/lo.2001.46.7.1684, 2001.

633 Dittmar, T., Cherrier, J. and Ludichowski, K. U.: The analysis of amino acids in seawater., in *Practical guidelines for*
634 *the analysis of seawater.*, edited by O. Wurl, pp. 67–78, CRC Press, Boca Raton., 2009.

635 Echevin, V., Aumont, O., Ledesma, J. and Flores, G.: The seasonal cycle of surface chlorophyll in the Peruvian
636 upwelling system : A modelling study, *Prog. Oceanogr.*, 79(2–4), 167–176, doi:10.1016/j.pocean.2008.10.026, 2008.

637 Engel, A. and Galgani, L.: The organic sea-surface microlayer in the upwelling region off the coast of Peru and

638 potential implications for air–sea exchange processes, *Biogeosciences*, 13(4), 989–1007, doi:10.5194/bg-13-989-
639 2016, 2016.

640 Engel, A. and Händel, N.: A novel protocol for determining the concentration and composition of sugars in
641 particulate and in high molecular weight dissolved organic matter (HMW-DOM) in seawater., *Mar. Chem.*, 127(1),
642 180–191, doi:10.1016/j.marchem.2011.09.004, 2011.

643 Engel, A., Thoms, S., Riebesell, U., Rochelle-Newall, E. and Zondervan, I.: Polysaccharide aggregation as a
644 potential sink of marine dissolved organic carbon, *Nature*, 428(6986), 929–932, doi:10.1038/nature02453, 2004.

645 Engel, A., Zondervan, I., Aerts, K., Beaufort, L., Benthien, A., Chou, L., Delille, B., Gattuso, J.-P., Harlay, J.,
646 Heemann, C., Hoffmann, L., Jacquet, S., Nejstgaard, J., Pizay, M.-D., Rochelle-Newall, E., Schneider, U.,
647 Terbrueggen, A. and Riebesell, U.: Testing the direct effect of CO₂ concentration on a bloom of the coccolithophorid
648 *Emiliana huxleyi* in mesocosm experiments, *Limnol. Oceanogr.*, 50(2), 493–507, doi:10.4319/lo.2005.50.2.0493,
649 2005.

650 Fischer, T., Banyte, D., Brandt, P., Dengler, M., Krahnemann, G., Tanhua, T. and Visbeck, M.: Diapycnal oxygen
651 supply to the tropical North Atlantic oxygen minimum zone, *Biogeosciences*, 10(7), 5079–5093, doi:10.5194/bg-10-
652 5079-2013, 2013.

653 Galán, A., Molina, V., Thamdrup, B., Woeikens, D., Lavik, G., Kuypers, M. M. M. and Ulloa, O.: Anammox bacteria
654 and the anaerobic oxidation of ammonium in the oxygen minimum zone off northern Chile, *Deep. Res. II*, 56, 1021–
655 1031, doi:10.1016/j.dsr2.2008.09.016, 2009.

656 Garreaud, R. D.: A plausible atmospheric trigger for the 2017 coastal El Niño, *Int. J. Climatol.*, 38, 1296–1302,
657 doi:10.1002/joc.5426, 2018.

658 Gasol, J. M. and Del Giorgio, P. A.: Using flow cytometry for counting natural planktonic bacteria and
659 understanding the structure of planktonic bacterial communities, *Sci. Mar.*, 64(2), 197–224,
660 doi:10.3989/scimar.2000.64n2197, 2000.

661 Goldman, J. C., Caron, D. A. and Dennett, M. R.: Regulation of gross growth efficiency and ammonium regeneration
662 in bacteria by substrate C : N ratio., *Limnol. Oceanogr.*, 32(6), 1239–1252, doi:10.4319/lo.1987.32.6.1239, 1987.

663 Graco, M. I., Purca, S., Dewitte, B., Castro, C. G., Morón, O., Ledesma, J., Flores, G. and Gutiérrez, D.: The OMZ
664 and nutrient features as a signature of interannual and low-frequency variability in the Peruvian upwelling system,
665 *Biogeosciences*, 14(20), 4601–4617, doi:10.5194/bg-14-4601-2017, 2017.

666 Grossart, H., Allgaier, M., Passow, U. and Riebesell, U.: Testing the effect of CO₂ concentration on the dynamics of
667 marine heterotrophic bacterioplankton, *Limnol. Oceanogr.*, 51(1), 1–11, doi:10.4319/lo.2006.51.1.0001, 2006.

668 Gruber, N.: Warming up, turning sour, losing breath : ocean biogeochemistry under global change., *Phil. Trans. R.*
669 *Soc.*, 369(143), 1980–1996, doi:10.1098/rsta.2011.0003, 2011.

- 670 Hadley Wickham: *ggplot2: Elegant Graphics for Data Analysis*, Springer-Verlag, New York., 2016.
- 671 Hoppe, H.-G.: Significance of exoenzymatic activities in the ecology of brackish water: measurements by means of
672 methylumbelliferyl-substrates., *Mar. Ecol. Prog. Ser.*, 11, 299–308, 1983.
- 673 Hoppe, H.-G., Gocke, K. and Kuparinen, J.: Effect of H₂S on heterotrophic substrate uptake, extracellular enzyme
674 activity and growth of brackish water bacteria., *Mar. Ecol. Prog. Ser.*, 64, 157–167, doi:10.3354/meps064157, 1990.
- 675 Hoppe, H.-G., Arnosti, C. and Herndl, G. F.: Ecological significance of bacterial enzymes in the marine
676 environment, in *Enzymes in the environment: activity, ecology, and applications*, edited by R. Burns and R. Dick,
677 pp. 73–108, Marcel Dekker, Inc., New York., 2002.
- 678 Hothorn, T., Bretz, F. and Westfall, P.: Simultaneous Inference in General Parametric Models, *Biometrical J.*, 50(3),
679 346–363, 2008.
- 680 Ilyina, T., Six, K. D., Segschneider, J., Maier-Reimer, E., Li, H. and Nunez-Riboni, I.: Global ocean biogeochemistry
681 model HAMOCC : Model architecture and performance as component of the MPI-Earth system model in different
682 CMIP5 experimental realizations, *J. Adv. Model. earth Syst.*, 5, 1–29, doi:10.1029/2012MS000178, 2013.
- 683 John Fox and Sanford Weisberg: *An {R} Companion to Applied Regression*, 2nd ed., SAGE Publications Ltd,
684 Thousand Oak {CA}., 2011.
- 685 Kalvelage, T., Jensen, M. M., Contreras, S., Revsbech, N. P., Lam, P., Günter, M., LaRoche, J., Lavik, G. and
686 Kuypers, M. M. M.: Oxygen sensitivity of anammox and coupled N-cycle processes in oxygen minimum zones,
687 edited by J. A. Gilbert, *PLoS One*, 6(12), e29299, doi:10.1371/journal.pone.0029299, 2011.
- 688 Kalvelage, T., Lavik, G., Lam, P., Contreras, S., Arteaga, L., Löscher, C. R., Oschlies, A., Paulmier, A., Stramma, L.
689 and Kuypers, M. M. M.: Nitrogen cycling driven by organic matter export in the South Pacific oxygen minimum
690 zone, *Nat. Geosci.*, 6(3), 228–234, doi:10.1038/ngeo1739, 2013.
- 691 Kalvelage, T., Lavik, G., Jensen, M. M., Revsbech, N. P., Löscher, C., Schunck, H., Desai, D. K., Hauss, H., Kiko,
692 R., Holtappels, M., LaRoche, J., Schmitz, R. A., Graco, M. I. and Kuypers, M. M. M.: Aerobic microbial respiration
693 in oceanic oxygen minimum zones, edited by Z.-X. Quan, *PLoS One*, 10(7), e0133526,
694 doi:10.1371/journal.pone.0133526, 2015.
- 695 Kämpf, J. and Chapman, P.: *Upwelling Systems of the World*, Springer International Publishing Switzerland, Cham.
696 [online] Available from: <http://link.springer.com/10.1007/978-3-319-42524-5>, 2016.
- 697 Kiko, R., Hauss, H., Buchholz, F. and Melzner, F.: Ammonium excretion and oxygen respiration of tropical
698 copepods and euphausiids exposed to oxygen minimum zone conditions, *Biogeoscience*, 13, 2241–2255,
699 doi:10.5194/bg-13-2241-2016, 2016.
- 700 Kirchman, D., K'nees, E. and Hodson, R.: Leucine incorporation and its potential as a measure of protein synthesis

701 by bacteria in natural aquatic systems., *Appl. Environm. Microbiol.*, 49(3), 599–607, 1985.

702 Kirchman, D. L., Rich, J. H. and Barber, R. T.: Biomass and biomass production of heterotrophic bacteria along
703 140°W in the equatorial Pacific: Effect of temperature on the microbial loop, *Deep Sea Res. Part II Top. Stud.*
704 *Oceanogr.*, 42(2–3), 603–619, doi:10.1016/0967-0645(95)00021-H, 1995.

705 Lam, P. and Kuypers, M. M. M.: Microbial nitrogen cycling processes in oxygen minimum zones., *Annu. Rev. Mar.*
706 *Sci.*, 3, 317–348, doi:10.1146/annurev-marine-120709-142814, 2011.

707 Lawson, C. E., Wu, S., Bhattacharjee, A. S., Hamilton, J. J., McMahon, K. D., Goel, R. and Noguera, D. R.:
708 Metabolic network analysis reveals microbial community interactions in anammox granules., *Nat. Commun.*,
709 8(15416), 1–12, doi:10.1038/ncomms15416, 2017.

710 Lee, C.: Controls on organic carbon preservation : the use of stratified water bodies to compare intrinsic rates of
711 decomposition in oxic and anoxic systems., *Geochim. Cosmochim. Acta*, 56(8), 3323–3335, doi:10.1016/0016-
712 7037(92)90308-6, 1992.

713 Lindroth, P. and Mopper, K.: High performance liquid chromatographic determination of subpicomole amounts of
714 amino acids by precolumn fluorescence derivatization with o-phthaldialdehyde., *Anal. Chem.*, 51(11), 1667–1674,
715 doi:10.1021/ac50047a019, 1979.

716 Llanillo, P. J., Karstensen, J. and Stramma, L.: Physical and biogeochemical forcing of oxygen and nitrate changes
717 during El Niño / El Viejo and La Niña / La Vieja upper-ocean phases in the tropical eastern South Pacific along 86 °
718 W, *Biogeosciences*, 10, 6339–6355, doi:10.5194/bg-10-6339-2013, 2013.

719 Llanillo, P. J., Pelegrí, J. L., Talley, L. D., Pena-Izquierdo, J. and Cordero, R. R.: Oxygen Pathways and Budget for
720 the Eastern South Pacific Oxygen Minimum Zone, *J. Geophys. Res.*, 123, 1722–1744, doi:10.1002/2017JC013509,
721 2018.

722 Loginova, A. N., Thomsen, S., Dengler, M., Lüdke, J. and Engel, A.: Diapycnal dissolved organic matter supply into
723 the upper Peruvian oxycline, *Biogeosciences*, 16, 2033–2047, doi:10.5194/bg-16-2033-2019, 2019.

724 López-Urrutia, Á. and Morán, X. A. G.: Resource limitation of bacterial production distorts the temperature
725 dependence of oceanic carbon cycling, *Ecology*, 88(4), 817–822, doi:10.1890/06-1641, 2007.

726 McDougall, T. J. and Barker, P. M.: Getting started with TEOS-10 and the Gibbs Seawater (GSW) oceanographic
727 toolbox, *SCOR/IAPSO WG 127*, , 28, 2011.

728 Van Mooy, B. A. S., Keil, R. G. and Devol, A. H.: Impact of suboxia on sinking particulate organic carbon:
729 Enhanced carbon flux and preferential degradation of amino acids via denitrification., *Geochim. Cosmochim. Acta*,
730 66(3), 457–465, doi:10.1016/S0016-7037(01)00787-6, 2002.

731 Pantoja, S., Rossel, P., Castro, R., Cuevas, L. A., Daneri, G. and Córdova, C.: Microbial degradation rates of small

732 peptides and amino acids in the oxygen minimum zone of Chilean coastal waters, *Deep Sea Res. Part*, 56(16), 1055–
733 1062, doi:10.1016/j.dsr2.2008.09.007, 2009.

734 Paulmier, A. and Ruiz-Pino, D.: Oxygen minimum zones (OMZs) in the modern ocean, *Prog. Oceanogr.*, 80(3–4),
735 113–128, doi:10.1016/j.pocean.2008.08.001, 2009.

736 Piontek, J., Sperling, M., Nöthig, E. M. and Engel, A.: Regulation of bacterioplankton activity in Fram Strait (Arctic
737 Ocean) during early summer: The role of organic matter supply and temperature., *J. Mar. Syst.*, 132, 83–94,
738 doi:10.1016/j.jmarsys.2014.01.003, 2014.

739 R Development Core Team: R: A language and environment for statistical computing, [online] Available from:
740 <http://www.r-project.org>, 2008.

741 Rivkin, R. B. and Legendre, L.: Biogenic carbon cycling in the upper ocean: Effects of microbial respiration,
742 *Science.*, 291(5512), 2398–2400, doi:10.1126/science.291.5512.2398, 2001.

743 Roullier, F., Berline, L., Guidi, L., Durrieu De Madron, X., Picheral, M., Sciandra, A., Pesant, S. and Stemmann, L.:
744 Particle size distribution and estimated carbon flux across the Arabian Sea oxygen minimum zone, *Biogeosciences*,
745 11(16), 4541–4557, doi:10.5194/bg-11-4541-2014, 2014.

746 Schafstall, J., Dengler, M., Brandt, P. and Bange, H.: Tidal-induced mixing and diapycnal nutrient fluxes in the
747 Mauritanian upwelling region, *J. Geophys. Res.*, 115(C10), C10014, doi:10.1029/2009JC005940, 2010.

748 Schlitzer, R.: *Ocean Data View*, 2016.

749 Simon, M. and Azam, F.: Protein content and protein synthesis rates of planktonic marine bacteria., *Mar. Ecol. Prog.*
750 *Ser.*, 51(3), 201–213, 1989.

751 Smith, D. C. and Azam, F.: A simple , economical method for measuring bacterial protein synthesis rates in seawater
752 using 3H-leucine, *Mar. Microb. Food Web*, 6(2), 107–114, 1992.

753 Steinfeldt, R., Sültenfuß, J., Dengler, M., Fischer, T. and Rhein, M.: Coastal upwelling off Peru and Mauritania
754 inferred from helium isotope disequilibrium, *Biogeoscience*, 12, 7519–7533, doi:10.5194/bg-12-7519-2015, 2015.

755 Stramma, L., Schmidtko, S., Levin, L. A. and Johnson, G. C.: Ocean oxygen minima expansions and their biological
756 impacts, *Deep Sea Res. Part I Oceanogr. Res. Pap.*, 57(4), 587–595, doi:10.1016/j.dsr.2010.01.005, 2010.

757 Strohm, T. O., Griffin, B., Zumft, W. G. and Schink, B.: Growth yields in bacterial denitrification and nitrate
758 ammonification, *Appl. Environ. Microbiol.*, 73(5), 1420–1424, doi:10.1128/AEM.02508-06, 2007.

759 Sugimura, Y. and Suzuki, Y.: A high-temperature catalytic oxidation method for the determination of non-volatile
760 dissolved organic carbon in seawater by direct injection of a liquid sample, *Mar. Chem.*, 24(2), 105–131,
761 doi:10.1016/0304-4203(88)90043-6, 1988.

- 762 Taylor, G. T., Thunell, R., Varela, R., Benitez-Nelson, C. and Scranton, M. I.: Hydrolytic ectoenzyme activity
763 associated with suspended and sinking organic particles within the anoxic Cariaco Basin, *Deep Sea Res. I*, 56(8),
764 1266–1283, doi:10.1016/j.dsr.2009.02.006, 2009.
- 765 Thamdrup, B., Dalsgaard, T. and Revsbech, N. P.: Widespread functional anoxia in the oxygen minimum zone of the
766 Eastern South Pacific, *Deep Sea Res. Part I Oceanogr. Res. Pap.*, 65, 36–45, doi:10.1016/j.dsr.2012.03.001, 2012.
- 767 Thrash, C. J., Seitz, K. W., Baker, B. J., Temperton, B., Gillies, L. E., Rabalais, N. N., Henrissat, B. and Mason, U.:
768 Metabolic roles of uncultivated bacterioplankton lineages in the northern Gulf of Mexico “Dead Zone,” *MBio*, 8(5),
769 1–20, doi:10.1128/mBio.01017-17, 2017.
- 770 Tiano, L., Garcia-Robledo, E., Dalsgaard, T., Devol, A. H., Ward, B. B., Ulloa, O., Canfield, D. E. and Peter
771 Revsbech, N.: Oxygen distribution and aerobic respiration in the north and south eastern tropical Pacific oxygen
772 minimum zones, *Deep Sea Res. Part I*, 94(October), 173–183, doi:10.1016/j.dsr.2014.10.001, 2014.
- 773 Ward, B. B.: How nitrogen is lost, *Science.*, 341(6144), 352–353, doi:10.1126/science.1240314, 2013.
- 774 Weiss, M., Abele, U., Weckesser, J., Welte, W., Schiltz, E. and Schulz, G.: Molecular architecture and electrostatic
775 properties of a bacterial porin, *Science.*, 254(5038), 1627–1630, doi:10.1126/science.1721242, 1991.
- 776 Winkler, W. L.: Die Bestimmung des im Wasser gelösten Sauerstoffes., *Berichte der Dtsch. Chem. Gesellschaft*,
777 21(2), 2843–2854, doi:10.1002/cber.188802102122, 1888.
- 778

779 **Figure legends**

780

781 **Figure 1:** Station map. All presented stations in the Eastern Tropical South Pacific off Peru sampled in 2017. For detailed
782 informations about the stations see supplementary Table 1.

783 **Figure 2:** Measured concentrations and calculated proxies for the change of dissolved organic carbon (DOC) and dissolved
784 oxygen (DO) flux over depth for stations G-T: The average diapycnal diffusivity of mass (K_ρ) over depth with confidence interval
785 and the constant $K_\rho (1 \times 10^{-3} m^2 s^{-1})$ that was used for further calculations (a). Concentrations of DOC in the upper 100 m and
786 the resulting change of DOC flux over depth ($\mathcal{F}\Phi$) (b). Concentrations of DO in the upper 100 m and the resulting change of DO
787 flux over depth ($\mathcal{F}\Phi$) (c).

788 **Figure 3:** Biotic and abiotic conditions at selected stations exemplary for the sampling conditions. Chlorophyll (a), temperature
789 (b), total dissolved nitrogen (TDN) (c), dissolved organic carbon (DOC) (d), carbon content of dissolved hydrolysable amino
790 acids (DHAA) (e) and carbon content of high molecular weight dissolved carbohydrates (DCHO) (f) over depth at different
791 stations from on- to offshore off Peru.

792 **Figure 4:** Bacterial growth activity at different *in situ* oxygen concentrations from on- to offshore off Peru during April 2017
793 (M136). Oxygen concentrations (a), total bacterial production (BP) (b), bacterial abundance (c) cell-specific BP (d) over the
794 upper 800 m depth with a zoom in the upper 100 m (small plots).

795 **Figure 5:** Extracellular enzyme rates at different *in situ* oxygen concentrations during April and June 2017 (M136, M138).
796 Oxygen concentrations (a), degradation rates of dissolved amino acids (DHAA) by leucine-aminopeptidase (LAPase) (b),
797 degradation rates of high molecular weight dissolved carbohydrates (DCHO) by β -glucosidase (GLUCase) (c) total potential
798 LAPase rates (V_{max}) (d), Glucose V_{max} (e), cell abundance (f), cell-specific degradation rates DHAA by LAPase (g), cell-specific
799 degradation rates of DCHO by GLUCase (h), cell-specific LAPase V_{max} (i) and cell-specific Glucose V_{max} (j) at different oxygen
800 regimes off Peru.

801

802

803

804 **Tables**

805 **Table 1:** Estimates of oxygen and DOC loss over depth based on *in situ* physical observations and bacterial rate measurements. Oxygen and DOC loss rates ($\text{mmol m}^{-3} \text{d}^{-1}$) were
806 estimated from the change in oxygen and DOC fluxes over depth. The bacterial uptake of DOC ($\text{mmol m}^{-3} \text{d}^{-1}$) was calculated from bacterial production ($\text{mmol m}^{-3} \text{d}^{-1}$) based on a
807 growth efficiency of 10 and 30% (DOC uptake_ϕ). The bacterial oxygen demand (BOD , $\text{mmol m}^{-3} \text{d}^{-1}$) and bacterial growth efficiency (BGE_ϵ , %) was calculated from bacterial
808 production and the assumption that DOC loss can be completely explained by bacterial uptake (BOD_ϵ) or estimated based on a BGE of 10 and 30% (BOD_ϕ).

809

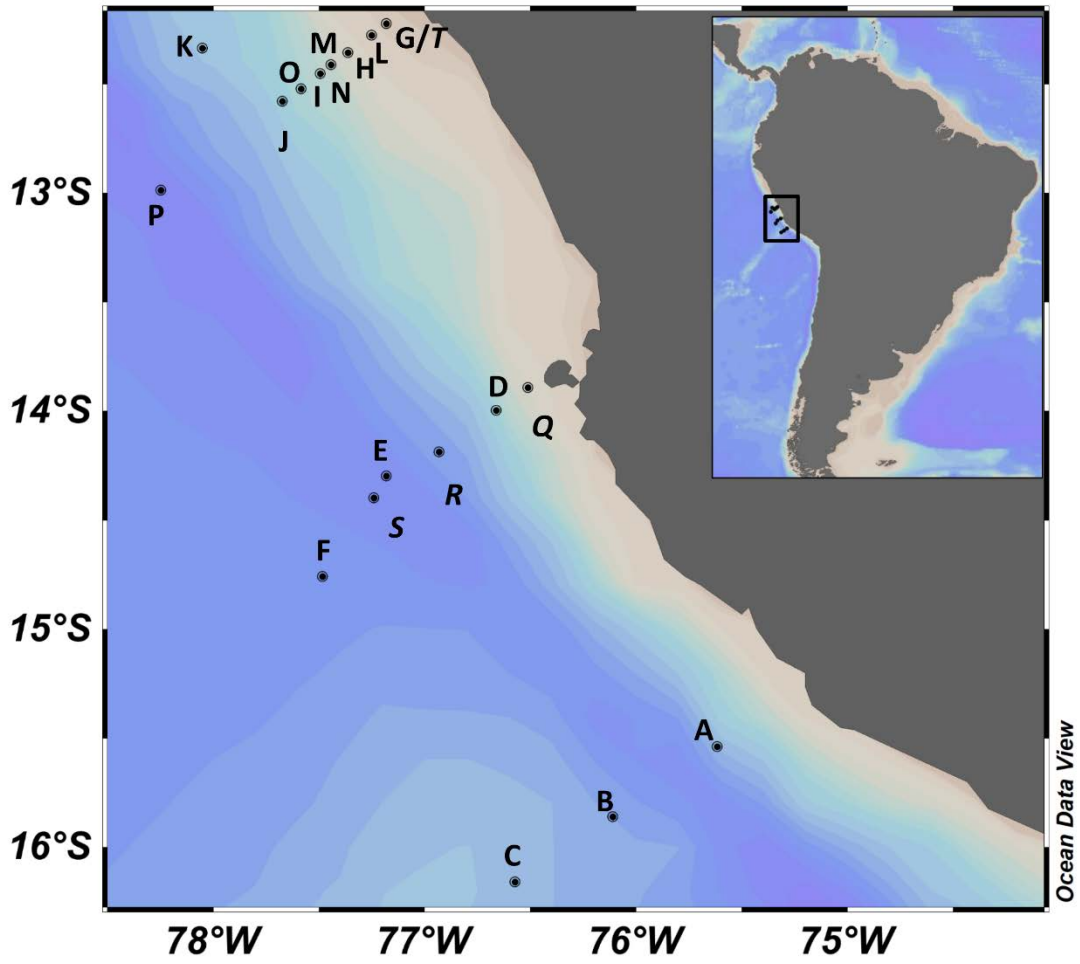
Depth	oxygen loss	DOC loss	DOCuptake $_{\phi 10}$			DOC uptake $_{\phi 30}$			Bacterial Production			BOD $_\epsilon$			BOD $_{\phi 10}$			BOD $_{\phi 30}$			BGE $_\epsilon$		
	avg	avg	avg	min	max	avg	min	max	avg	min	max	avg	min	max	avg	min	max	avg	min	max	avg	min	max
MLD-40	10.23	3.4	2.22	0.35	7.10	0.74	0.12	2.37	0.22	0.03	0.71	3.17	2.68	3.36	2.00	0.31	6.39	0.52	0.08	1.66	6.55	1.02	20.92
40-60	5.55	1.13	0.56	0.25	1.46	0.19	0.08	0.49	0.06	0.03	0.15	1.07	0.98	1.10	0.51	0.23	1.32	0.13	0.06	0.34	5.00	2.26	12.97

810

811

812

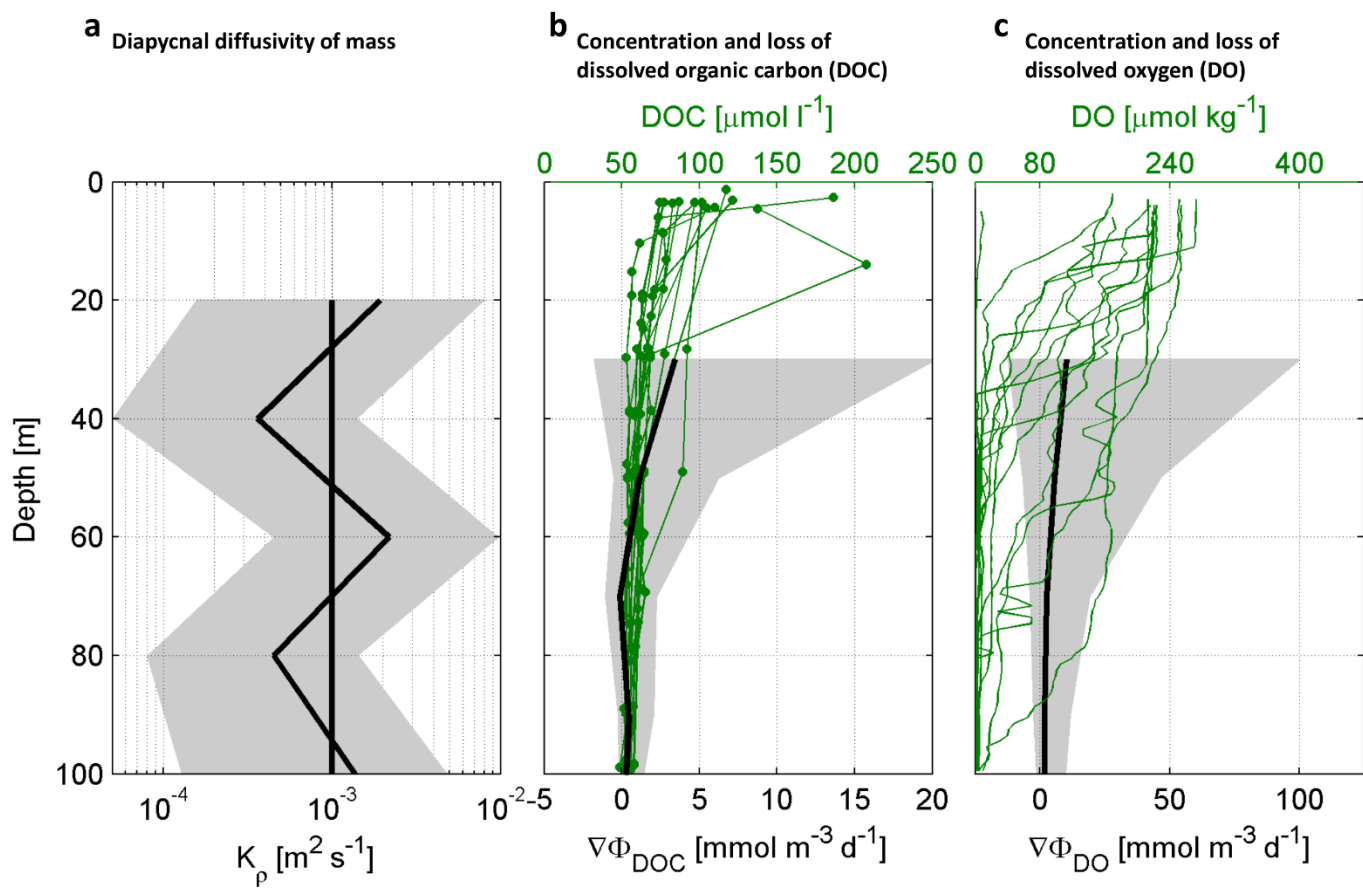
813 **Figures**



814

815 **Figure 1**

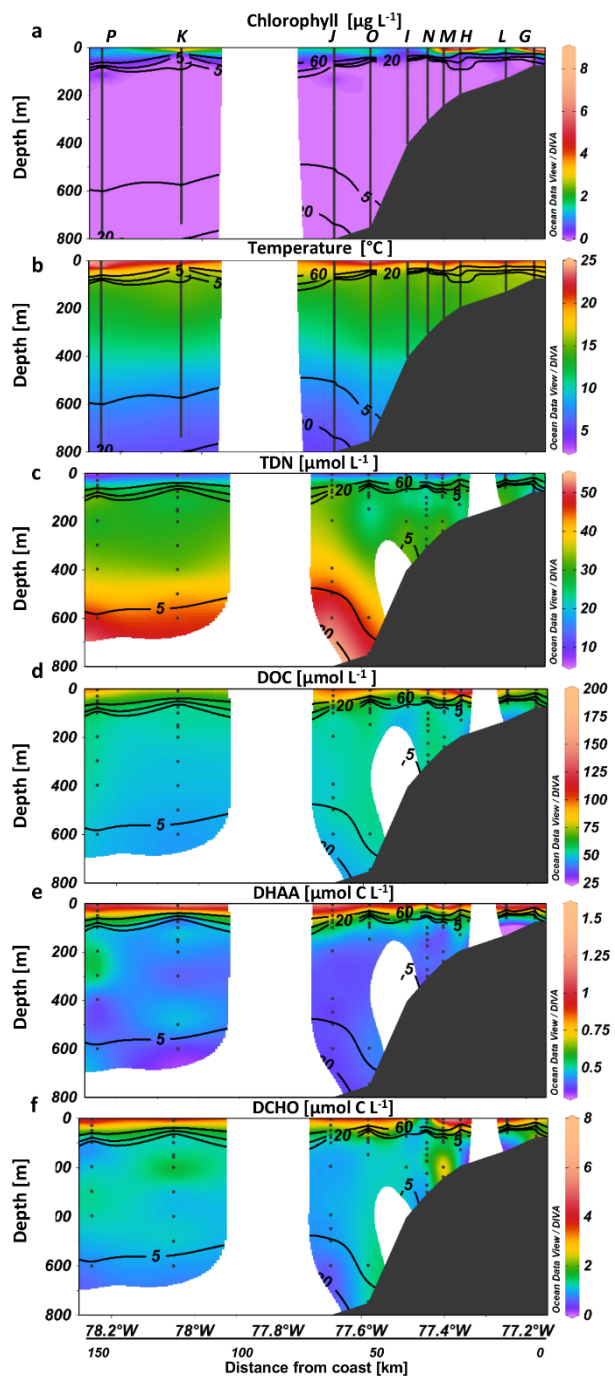
816



817

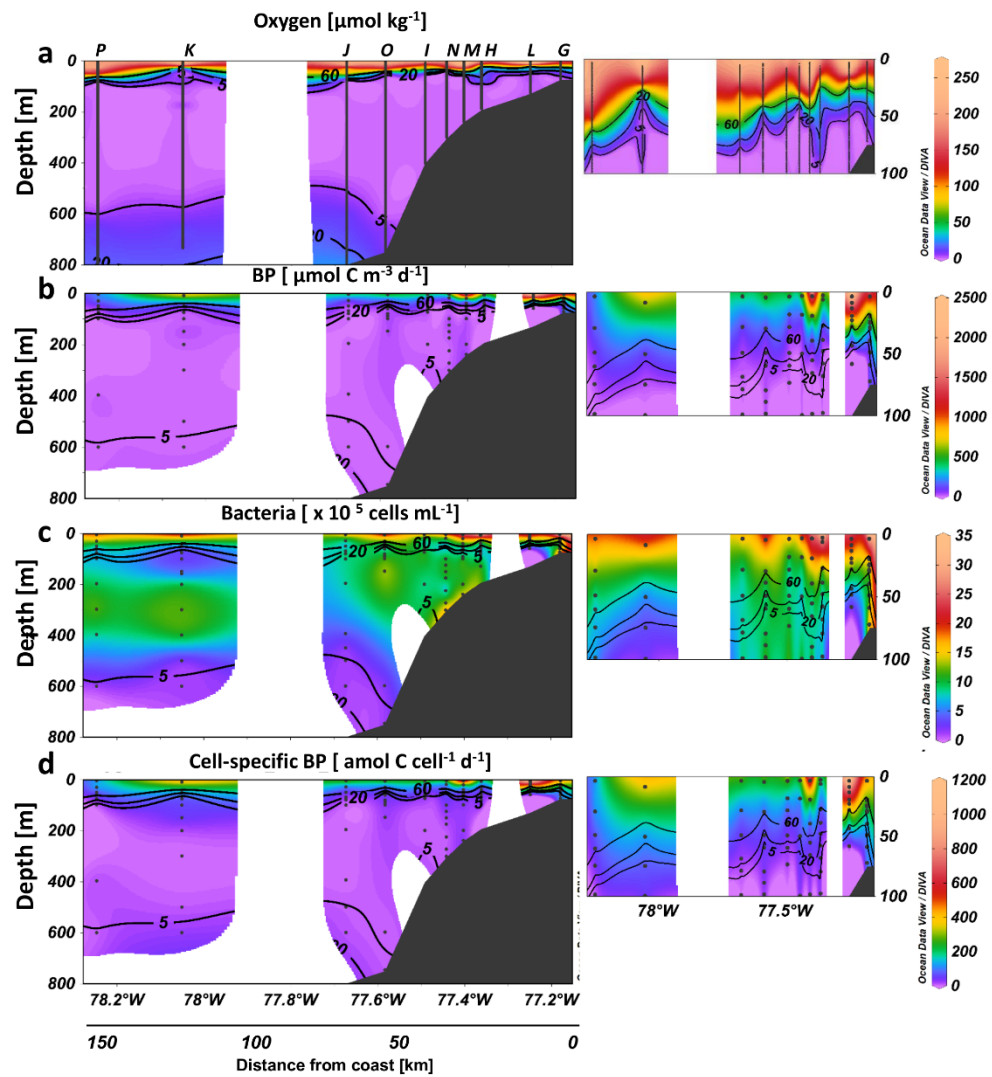
818 **Figure 2**

819



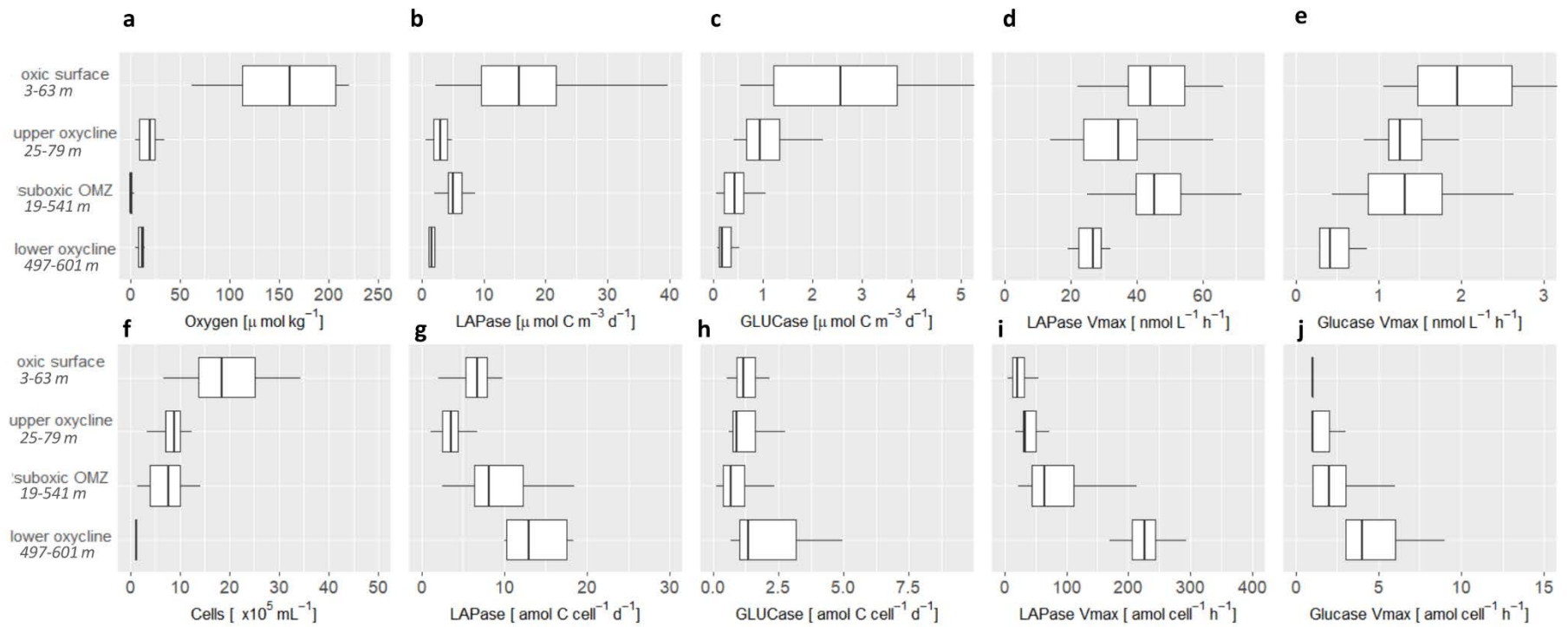
820

821 **Figure 3**



822

823 **Figure 4**



824

825 **Figure 5**

826

827

828

829